KAUNAS UNIVERSITY OF TECHNOLOGY

IRYNA HLADKA

SYNTHESIS AND STUDIES OF NEW ORGANIC ELECTROACTIVE COMPOUNDS CONTAINING DONOR AND ACCEPTOR MOIETIES

DOCTORAL DISSERTATION

Technological Sciences, Materials Engineering (T 008)

2020, Kaunas

This doctoral dissertation was prepared at Kaunas University of Technology, Faculty of Chemical Technology, Department of Polymer Chemistry and Technology during the period of 2015–2019. The studies were supported by the Research Council of Lithuania.

Scientific Supervisor:

Prof. Habil. Dr. Juozas Vidas GRAŽULEVIČIUS (Kaunas University of Technology, Technological sciences, Materials Engineering T 008).

Scientific Advisor:

Dr. Dmytro VOLYNIUK (Kaunas University of Technology, Natural Sciences, Chemistry, N 003).

Editor:
Dr. Armandas Rumšas (Publishing Office "Technologija")
Aurelija Gražina Rukšaitė (Publishing Office "Technologija").

Dissertation Defence Board of Material Engineering Scientific Field:
Prof. Dr. Habil. Sigitas TAMULEVIČIUS (Kaunas University of Technology, Technological sciences, Materials Engineering, T 008) – **chairman**;
Dr. Mindaugas ANDRULEVIČIUS (Kaunas University of Technology, Technological sciences, Materials Engineering, T 008);
Prof. Dr. Saulius GRIGALEVIČIUS (Kaunas University of Technology, Technological sciences, Materials Engineering, T 008);
Prof. Habil. Dr. Vidmantas GULBINAS (Centre for Physical Sciences and Technology, Natural Sciences, Physics, N 002);
Prof. Dolores VELASCO (University of Barcelona, Natural Sciences, Chemistry, N 003).

The official defence of the dissertation will be held at 12:30 p.m. on 9th of March, 2020 at the public meeting of the Dissertation Defence Board of Materials Engineering Scientific Field at the Rectorate Hall at Kaunas University of Technology.

Address: K. Donelaičio St. 73-402, 44249, Kaunas, Lithuania.
Phone: (+370) 37 300 042; fax: (+370) 37 324 144; email: doktorantura@ktu.lt

This doctoral dissertation was sent out on 9th February 2020.
The doctoral dissertation is available on the internet at http://ktu.edu and at the library of Kaunas University of Technology (K. Donelaičio St. 20, 44239, Kaunas, Lithuania).

The bibliographic information about the publication is available at the National Bibliographic Data Bank (NBDB) of the Martynas Mažvydas National Library of Lithuania.

KAUNAS UNIVERSITY OF TECHNOLOGY

IRYNA HLADKA

ORGANINIŲ ELEKTROAKTYVIŲ JUNGINIŲ, SUDARYTŲ IŠ DONORINIŲ IR AKCEPTORINIŲ FRAGMENTŲ, SINTEZĖ IR TYRIMAI

DAKTARO DISERTACIJA

Technologijos mokslai, Medžiagų inžinerija (T 008)

2020, Kaunas

Disertacija rengta 2015-2019 metais Kauno technologijos universiteto Cheminės technologijos fakultete, Polimerų chemijos ir technologijos katedroje. Mokslinius tyrimus rėmė Lietuvos mokslo taryba.

Mokslinis vadovas:

Prof. habil dr. Juozas Vidas GRAŽULEVIČIUS (Kauno technologijos universitetas, technologijos mokslai, Medžiagų inžinerija T 008).

Mokslinis konsultantas:

Dr. Dmytro VOLYNIUK (Kauno technologijos universitetas, gamtos mokslai, Chemija, N 003).

Redagavo:
Dr. Armandas Rumšas (leidykla "Technologija").
Aurelija Gražina Rukšaitė (leidykla "Technologija").

Medžiagų inžinerijos mokslo krypties disertacijos gynimo taryba:
Prof. habil dr. Sigitas TAMULEVIČIUS (Kauno technologijos universitetas, technologijos mokslai, Medžiagų inžinerija, T 008) – **pirmininkas**;
Dr. Mindaugas ANDRULEVIČIUS (Kauno technologijos universitetas, technologijos mokslai, Medžiagų inžinerija, T 008);
Prof. dr. Saulius GRIGALEVIČIUS (Kauno technologijos universitetas, technologijos mokslai, Medžiagų inžinerija, T 008);
Prof. habil. dr. Vidmantas GULBINAS (Fizinių ir technologijos mokslų centras, gamtos mokslai, Fizika, N 002);
Prof. Dolores VELASCO (Barselonos universitetas, gamtos mokslai, Chemija, N 003).

Disertacija bus ginama viešame chemijos mokslo krypties disertacijos gynimo tarybos posėdyje 2020 m. kovo 9 d. 12:30 val. Kauno technologijos universiteto Rektorato salėje.

Adresas: K. Donelaičio g. 73-402, 44249 Kaunas, Lietuva.
Tel. (370) 37 300 042; faks. (370) 37 324 144; el. paštas doktorantura@ktu.lt

Disertacija išsiųsta 2020 m. vasario 9 d. Su disertacija galima susipažinti internetinėje svetainėje http://ktu.edu ir Kauno technologijos universiteto bibliotekoje (K. Donelaičio g. 20, 44239 Kaunas).

Leidinio bibliografinė informacija pateikiama Lietuvos nacionalinės Martyno Mažvydo bibliotekos Nacionalinės bibliografijos duomenų banke (NBDB).

LIST OF ABBREVIATIONS

ACQ	Aggregation-caused quenching
AIE	Aggregation-induced emission
CE/η_c	Current efficiency
CELIV	Charge extraction by linearly increasing voltage technique
CIE	Commission Internationale de l'Eclairage
CT	Charge transfer
CV	Cyclic voltammetry
D-A	Donor-acceptor
D-A-D	Donor-acceptor-donor
DF	Delayed fluorescence
DFT	Density functional theory
DSC	Differential scanning calorimetry
EA_{CV}	Electron affinity measured by CV
EA_{PE}	Electron affinity measured by photoelectron emission method
EL	Electroluminescent
EQE/ η_{ext}	External quantum efficiency
E_S	Energy of singlet state
E_T	Energy of triplet state
ETM	Electron transporting materials
FIrpic	Iridium(III)bis(4,6-di-fluorophenyl)-pyridinato-N,C2')picolinate
HOMO	Highest occupied molecular orbital
HTM	Hole transporting materials
ICT	Intramolecular charge transfer
IP_{CV}	Ionization potential measured by CV
IP_{PE}	Ionization potential measured by photoelectron emission method
IQE	Internal quantum efficiency
ITO	Indium-tin oxide
LUMO	Lowest unoccupied molecular orbital
MCL	Mechanochromic luminescence
mCP	1,3-Bis(N-carbazolyl)benzene
Me	Methyl
MoO_3	Molybdenum trioxide
MS	Mass spectrometry
NMR	Nuclear magnetic resonance
NPB	N,N'-Di(1-naphthyl)-N,N'-diphenyl-(1,1'-biphenyl)-4,4'-diamine
OLEDs	Organic light-emitting diodes
OPVs	Organic photovoltaic cells
PE/η_p	Power efficiency

PFBP	Perfluorobiphenyl
PhOLEDs	Phosphorescent organic light-emitting diodes
PLQY	Photoluminescence quantum yield
RISC	Reversed intersystem crossing
TADF	Thermally activated delayed fluorescence
T_{cr}	Temperature of crystallization
TCTA	Tris(4-(carbazol-9-yl)phenyl)amine
TCz1	3,6-Bis(carbazol-9-yl)-9-(2-ethyl-hexyl)-9*H*-carbazole
TGA	Thermogravimetric analysis
T_{ID}	Temperature of 5% weight loss
T_m	Melting temperature
TOF	Time-of-flight
TPBi	2,2',2''-(1,3,5-Benzinetriyl)-tris(1-phenyl-1-*H*-benzimidazole)
TSPO1	Diphenyl[4-(triphenylsilyl)phenyl]phosphine oxide
TTA	Triplet-triplet annihilation
UV-VIS	Ultraviolet-visible
ΔE_{S-T}	Singlet-triplet energy gap
Δf	Orientation polarizability of solvents
$\lambda_{abs}/\lambda_{em}$	Wavelength of maximum absorption/emission
τ	Excited-state lifetime
χ^2	Values of the accuracy of experiment
Φ	Quantum yield

Table of Contents

1. INTRODUCTION

Flexible and non-flexible displays for smartphones and TV screens, colored light sources and portable solar cells are examples of irreplaceable optoelectronic devices with a wide application for everyday usage[1,2]. Utilization of organic semiconductors for the fabrication of organic light-emitting diodes (OLEDs) and organic as well as hybrid photovoltaic cells has increased in the last two decades[3]. The OLED technology has become extremely demanded due to the wide application potential of OLEDs in display panels for computers, smartphones, wearable electronics and TV panels as well as lightning devices since their first commercialization in 1997[4]. Despite the evident advantages of OLEDs (low cost of production, thinness of displays, flexibility, incredible contrast ratio, a wide viewing angle and color gamut, etc.), there are still many shortcomings (device degradation, and, as a result, a short working lifetime, insufficient efficiency of blue devices) which are still required to be solved. High performance of organic electroluminescent devices can be achieved by combination of the development of new organic materials together with the optimization of the structures of the devices.

The basic OLEDs structure consists of a thin layer of an organic material sandwiched between the cathode and the anode[5]. A facile, balanced charge transport and high conversion efficiency of excitons to light are required for a successful OLED[6]. To achieve an efficient recombination of holes and electrons in the emitting layer, a π-conjugated structure of organic electroluminescent materials is required. Also, suitable optical and photophysical properties, good thermal and morphological stability, as well as appropriate energy levels are the main requirements for organic electroactive materials intended for the fabrication of highly efficient electroluminescent devices. A combination of different donor (D) and acceptor (A) moieties in the structures of organic semiconductors makes possible to achieve a big range of desired properties[3]. Careful design and synthesis of multifunctional organic materials together with device structure optimization makes it possible to obtain highly efficient OLEDs.

One of the approaches towards enhancing the device efficiency is the exploitation of phosphorescent emission. It is well known that during the charge carrier recombination in the emissive layer, singlet and triplet excitons are formed at a ratio of 1:3, respectively. Thus, the maximum of internal quantum efficiency (IQE) of only 25% can be reached by use of fluorescent emitters. However, 100% IQE can be realized by using organometallic complexes containing transition metals due to the harvesting of singlet and triplet excitons[7].

Another approach towards achieving a high efficiency of PhOLEDs is the development of effective host materials. In general, good host materials meet the main requirements[8,9,10,11], such as: a higher triplet energy level than that of the dopant emitter in order to avoid reverse energy transfer from the guest back to the host; balanced charge carrier transport for the recombination of holes and electrons and the restriction of the exciton formation zone in the emissive layer; matching the highest occupied/lowest unoccupied molecular orbitals (HOMO/LUMO) of the neighboring layers in order to reduce the driving voltage of the device; good thermal and morphological stabilities while seeking to enhance the operation lifetime of devices.

Commonly, a bulky and sterically hindered molecular configuration is desirable for increasing the glass transition temperature (T_g) and the formation of morphologically stable and homogenous amorphous films[12]. Highly efficient bipolar host materials for OLED fabrication can be designed by a combination of hole- and electron-transporting units in a single molecule. Carbazole-based derivatives are widely used as host materials due to good hole-transporting characteristics, high triplet energy[13,14], and a possibility of functionalization at the 9th position[15]. Such moieties as triazine[16,17,18], pyridine[19,20], benzimidazole[21,22,23] and oxadiazole[24,25,26] have been used as electron accepting units in the synthesis of bipolar host materials. Wide utilization of oxadiazole-based derivatives for an increase of external quantum efficiency of electroluminescence devices is based on good thermal stability and high electron mobility[27,28]. Thus, a combination of carbazole and oxadiazole moieties in a single molecular structure offers a possibility to obtain efficient bipolar host semiconductors for PhOLED fabrication.

The third approach towards enhancing OLED efficiency is the implementation of compounds exhibiting delayed fluorescence (DF). The DF mechanism is based on the total utilization of triplet excitons over up-conversion of nonradiative triplet states into radiative singlet states[29]. DF can be divided into two types: *triplet-triplet annihilation* (TTA), i.e., the so-called P-type emission, and *thermally activated delayed fluorescence* (TADF), also known as the E-type emission. In the TTA process, two excited triplet (T_1) states produce one singlet (S_1) excited state during the up-conversion process. As a result, the IQE of OLEDs can be increased to 37.5% by the production of additional singlet excitons. Moreover, the addition of the prompt fluorescence emission component enhances the total IQE up to 62.5%. Another way of the up-conversion process is the TADF mechanism which can be realized through the reverse intersystem crossing (RISC) process with 100% efficiency of triplet state harvesting[30]. The E-type fluorescence mechanism occurs due to the harvesting of all the triplet excitons from the locally excited triplet state $T_{1(LE)}$ by conversion to the locally excited singlet state $S_{1(LE)}$ resulting in a longer decay time in comparison to prompt fluorescence with the same spectral wavelength[31]. The efficient RISC process depends on two main requirements: the minimization of energy splitting between the singlet and the triplet excited states ($\Delta E_{S\text{-}T}$) and the achievement of high photoluminescence quantum yields and long lifetimes of the excited triplet state by suppression of nonradiative pathways, which is possible for the excited singlet and triplet states[32].

A small value of $\Delta E_{S\text{-}T}$, the spatial separation of HOMO/LUMO with a small overlap, an efficient RISC process, good electrochemical and thermal properties, and the high morphological stability of the layers are the main requirements for the achievement of an effective TADF mechanism[33,34]. To achieve the above-mentioned parameters, a careful structural design has to be implemented. A bipolar molecular structure resulting in the internal charge transfer is required to realize TADF. A small $\Delta E_{S\text{-}T}$ value can be achieved by the rigid regulation of the torsion angle between the electron-donating and the electron-accepting units, or between HOMO and LUMO. The design strategy of efficient TADF emitters mainly concentrated on sp^3-hybridized nitrogen-containing aromatic heterocycles (carbazole, phenothiazine, phenoxazine,

acridan, etc.) due to their good thermal and electrochemical stability, good hole-transporting properties, a strong electron-donating ability, and stable and high triplet states of the derivatives. An array of electron-withdrawing functional groups and heterocycles, such as nitrile, pyrimidine, pyridine, oxadiazole, triazole, benzophenone, etc., are suitable candidates for the usage in bipolar molecules for efficient TADF emitters. As a result, a combination of different donor and acceptor fragments through various possibilities of their linkage ensures a high flexibility of the synthesis of derivatives for the potential usage in TADF OLEDs.

A modification of the molecular structure of organic fluorescent materials is an opportunity for controlling their properties, especially the color of emission, with the resulting influence of mechanochromism and polymorphism[35]. Some organic compounds are able to form several types of crystals with different molecular packing and geometries and exhibit various solid-state fluorescence[36,37]. It is known that the photophysical properties of organic electroactive compounds are strongly dependent on the molecular distribution in the solid state[38,39]. The usage of polymorphic materials is the promising approach towards obtaining derivatives with specific luminescent properties. Meanwhile, mechanochromic luminescent (MCL) materials are characterized by the reversibly changeable color of emission under external stimuli including mechanical forces, fuming of solvents, temperature gradient, and electric field[35,40,41,42].

Despite the rapid development of the field of organic optoelectronics and the huge number of organic electroactive materials, some critical issues, such as expensive production, high roll-off, and a short working lifetime, especially for deep blue-emitting devices, should still be solved. Therefore, synthesis of novel efficient multifunctional materials which could be applied as emitters, hosts, electron- (ETM) or hole-transporting materials (HTM), and profound understanding of structure-properties relationships is still required for obtaining compounds with enhanced characteristics. Preparation of multifunctional materials characterized by the required specific properties is a complicated challenge which is based on a careful choice of the donating and accepting units and the spacers between them. The careful selection of the appropriate moieties can result in efficient host materials with high triplet energies, good hole and electron transporting properties, and in effective luminescence. Emitters characterized by TADF, aggregation-induced emission (AIE), polymorphism and mechanochromism or their combinations are of greatest interest. Thus, multifunctional organic compounds are promising candidates for the enhancement of performance of electroluminescent devices, especially for blue OLEDs.

The aim of this work is the design, synthesis and investigation of properties of new donor-acceptor organic derivatives for potential application in OLEDs.

To achieve the aim of the thesis, the following tasks are formulated:

• Synthesis of carbazole and oxadiazole derivatives as high-triplet-energy host materials for OLEDs.

• Synthesis of acridan substituted perfluorobiphenyl derivatives as blue/sky-blue TADF emitters for OLEDs.

• Investigation of the properties of the synthesized compounds by experimental and computational methods.

• Investigation of the structure-properties relationships of derivatives containing acridan and perfluorobiphenyl moieties.

• Investigation of photophysical and electrochemical properties of new organoboron complexes.

• Estimation of the possibilities of application of the synthesized materials in electroluminescent devices.

The novelty of the work:

• New carbazole-oxadiazole donor-acceptor host materials for OLEDs were designed, synthesized, characterized and applied in phosphorescent OLED.

• New polymorphic derivatives of acridan and perfluorobiphenyl exhibiting thermally activated delayed fluorescence and aggregation-induced emission enhancement were designed, synthesized, characterized and applied in TADF OLEDs.

• The influence of donor and acceptor substituents attached to a benzothiazole fragment on the photophysical properties of the new families of highly emissive organoboron complexes were investigated.

Personal input of the author

The author has designed, synthesized and purified two different series of bipolar organic semiconductors described in Chapters 2.1 and 2.2. The author has performed and analyzed the results of theoretical calculations, structure analysis, UV-VIS absorption, and photoluminescence including quantum yield and excited-state lifetime and cyclic voltammetry measurements. Dr. Roman Lytvyn (Department of Polymer Chemistry and Technology, Kaunas University of Technology; Department of Organic Chemistry, Ivan Franko National University of Lviv) advised on molecular design, synthesis and structural confirmation. Measurements of the mass spectra were performed by dr. Dalius Gudeika (Department of Polymer Chemistry and Technology, Kaunas University of Technology); the results were further analyzed by the author. Electron photoemission measurements, charge mobility measurements, fabrication and characterization of OLEDs were done by dr. Dmytro Volyniuk and Mr. Oleksandr Bezvikonnyi (Department of Polymer Chemistry and Technology, Kaunas University of Technology); the results were further analyzed by the author. The measurements and discussion of the results of the X-ray Powder Diffraction spectra, Atomic Force Microscopy and X-ray Diffraction Measurement at Grazing Incidence were performed by dr. Algirdas Lazauskas (Institute of Materials Science, Kaunas University of Technology). The measurements of single crystal X-ray diffraction analysis were done by dr. Vasyl Kinzhybalo and dr. Tamara J. Bednarchuk (Institute of Low Temperature and Structure Research, Polish Academy of Sciences); the results were further analysed by dr. Vasyl Kinzhybalo in collaboration with the author and dr. Yan Danyliv (Department of Polymer Chemistry and Technology, Kaunas University of Technology). The organic materials described in Chapter 2.3 were designed, synthesized and analyzed by dr. Mykhaylo A. Potopnyk (Institute of

Organic Chemistry, Polish Academy of Sciences). The author has performed and processed the obtained results of UV-VIS absorption and photoluminescence including quantum yield and cyclic voltammetry measurements. The measurements of excited-state lifetimes and the processing of the results of the measurements were performed by dr. Yan Danyliv. Dr. Piotr Cmoch (Institute of Organic Chemistry, Polish Academy of Sciences) performed NMR measurements and analyzed the NMR spectra of fluorinated compounds, including the two-dimensional spectra. The measurements of single crystal X-ray diffraction analysis and the transcription of all the X-ray structures was done by dr. Magdalena Ceborska and dr. Roman Luboradzki (Institute of Physical Chemistry, Polish Academy of Sciences). Prof. dr. Habil. Juozas Vidas Gražulevičius (Department of Polymer Chemistry and Technology, Kaunas University of Technology) advised on the synthesis of bipolar organic semiconductors and the preparation of articles.

List of scientific publications on the topic of the dissertation

1. Hladka, Iryna; Lytvyn, Roman; Volyniuk, Dmytro; Gudeika, Dalius; Grazulevicius, Juozas V. W-shaped bipolar derivatives of carbazole and oxadiazole with high triplet energies for electroluminescent devices // Dyes and pigments. ISSN 0143-7208. 2018, vol. 149, p. 812-821. [Web of Science]. https://www.sciencedirect.com/science/article/pii/S0143720817317904

2. Hladka, Iryna; Volyniuk, Dmytro; Bezvikonnyi, Oleksandr; Kinzhybalo, Vasyl; Bednarchuk, Tamara J.; Danyliv, Yan; Lytvyn, Roman; Lazauskas, Algirdas; Gražulevičius, Juozas Vidas. Polymorphism of derivatives of *tert*-butyl substituted acridan and perfluorobiphenyl as sky-blue OLED emitters exhibiting aggregation induced thermally activated delayed fluorescence // Journal of materials chemistry C. ISSN 2050-7526. 2018, vol. 6, iss. 48, p. 13179-13189. [Web of Science]. https://pubs.rsc.org/en/content/articlelanding/2018/tc/c8tc04867c#!divAbstract

3. Potopnyk, Mykhaylo A.; Volyniuk, Dmytro; Ceborska, Magdalena; Cmoch, Piotr; Hladka, Iryna; Danyliv, Yan; Gražulevičius, Juozas Vidas. Benzo[4,5]thiazolo[3,2-*c*][1,3,5,2]oxadiazaborinines: synthesis, structural, and photophysical properties // Journal of organic chemistry. ISSN 0022-3263. 2018, vol. 83, iss. 19, p. 12129-12142. [Web of Science]. https://pubs.acs.org/doi/10.1021/acs.joc.7b01122

4. Potopnyk, Mykhaylo A.; Volyniuk, Dmytro; Luboradzki, Roman; Ceborska, Magdalena; Hladka, Iryna; Danyliv, Yan; Gražulevičius, Juozas Vidas. Application of the Suzuki-Miyaura reaction for the postfunctionalization of the benzo[4,5]thiazolo[3,2-*c*][1,3,5,2]oxadiazaborinine core: an approach toward fluorescent dyes // Journal of organic chemistry. ISSN 0022-3263. 2019, vol. 84, iss. 9, p. 5614-5626. [Web of Science]. https://pubs.acs.org/doi/10.1021/acs.joc.9b00566

2. RESULTS AND DISCUSSION

2.1. Synthesis and investigation of W-shaped carbazole-oxadiazole derivatives (Scientific publication No. 1, Q1, 12 quotations)

This chapter is based on the paper published in *Dyes Pigm.*, **2018**, *149*, 812–821[43]. Bipolar host materials with high triplet energy values based on carbazole and oxadiazole moieties were designed and synthesized. A synthetic pathway and chemical structures of obtained derivatives **1–4** are presented in Scheme 2.1. The synthetic approach based on temperature-induced recyclization reactions of *in situ* formed diacylbenzeneditetrazoles to phenylenedioxadiazoles was used to obtain the target derivatives. The chemical structures of synthesized compounds **1–4** were characterized by ^{1}H and ^{13}C NMR spectroscopy and mass spectrometry.

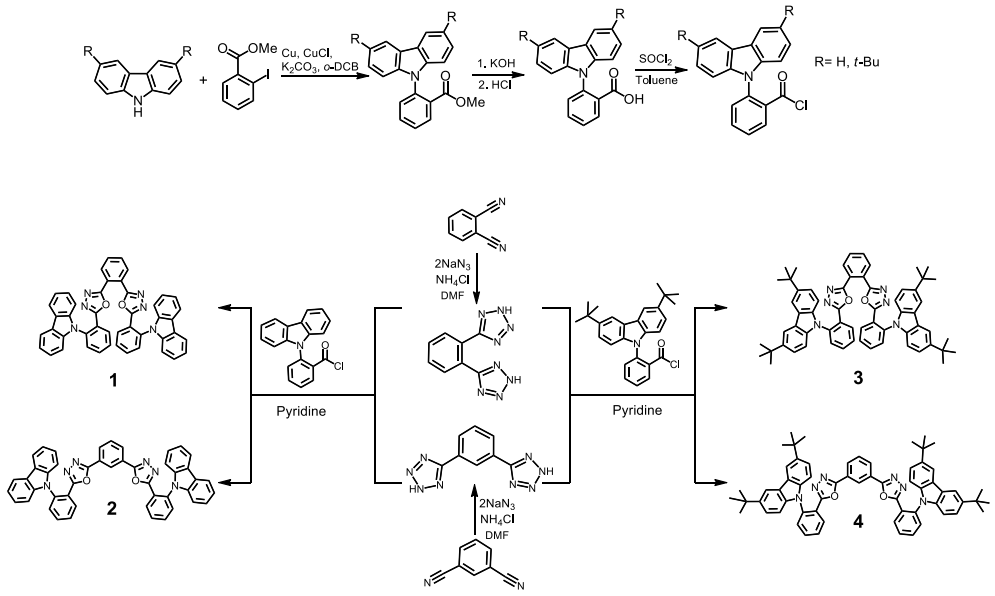

Scheme 2.1. Synthetic pathway

Theoretical calculations of the carbazole-oxadiazole containing derivatives were performed by using the density function theory (DFT) method via Spartan'14 software package[44]. The geometries of the molecular structures were optimized at B3LYP functional level with 6–31+G* basis set in vacuum. The DFT-optimized geometries of compounds **1–4** with the localization of the frontier molecular orbitals of these compounds and their energies are shown in Fig. 2.1. The HOMO and LUMO orbitals are generally separated and located on carbazole and phenyldioxazolyl fragments, respectively.

The thermal stability and the morphological properties of compounds **1–4** were investigated by thermogravimetric analysis (TGA) and differential scanning calorimetry (DSC) techniques. The temperatures of 5% weight loss (T_{ID}), melting point (T_m), and glass transitions (T_g) are summarized in Table 2.1. All the synthesized derivatives were isolated after the synthesis and purification as crystalline materials

and showed endothermic melting signals from the first scan, T_m values were found to be in the range from 163 °C to 264 °C (Table 2.1). *Tert*-butyl-substituted carbazole-based derivatives (**3** and **4**) are characterized by higher T_{ID} (by 16 °C) and T_g (by 30–33 °C) values, in comparison with the materials having unsubstituted carbazolyl moieties (**1** and **2**). The addition of *tert*-butyl groups increased the molecular weight of **3** and **4** and resulted in higher T_{ID} and T_g.

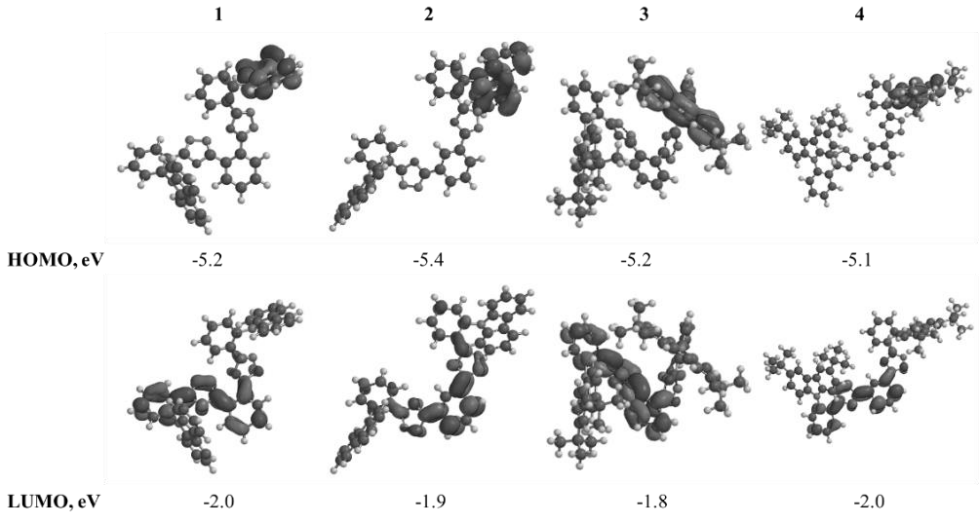

Fig. 2.1. Frontier orbitals distribution and their energies for compounds **1–4**

Table 2.1. Thermal, optical and photophysical characteristics of compounds **1–4**

Comp.	T_{ID} [a], °C	T_m [b], °C	T_g [b], °C	λ_{abs} [c/d/e], nm	λ_{PL} [d/e/f], nm	Φ_{PL} [d]	Φ_{PL} [f]	E_S, eV	E_T, eV	ΔE_{S-T}
1	359	251	107	335/338 /337	429/427 /439	0.15	0.22	3.33	3.04	0.29
2	367	163	110	336/338 /337	427/445 /427	0.09	0.24	3.30	3.04	0.26
3	375	264	147	342/343 /344	442/440 /470	0.15	0.08	3.13	2.97	0.16
4	383	257	143	342/342 /342	443/438 /456	0.16	0.12	3.14	2.97	0.19

[a] Determined by TGA. [b] Determined by DSC. λ_{abs} is the wavelength of absorption maximum; λ_{PL} is the wavelength of photoluminescence emission maximum; Φ is photoluminescence quantum yield. [c] Dichloromethane solution. [d] Solid state. [e] Toluene solution. [f] THF solution. E_S, E_T are the energies of singlet and triplet levels, respectively.

The absorption and photoluminescence (PL) spectra of dilute solutions and thin films are shown in Fig. 2.2. The absorption peaks of the intramolecular charge transfer of solutions and of solid films of compounds **1–4** were found to be in the region of 335–344 nm (Table 2.1). All the synthesized derivatives are characterized by blue emission in toluene solutions and thin films, and by bathochromically-shifted emission in THF solutions. The low polarity of the synthesized carbazole-oxadiazole based derivatives resulted in very close values of the emission maxima in solid layers

and toluene solutions. The bathochromic shifts of the PL spectra of the target derivatives in THF solutions are probably related to the solvatochromic effect conditioned by intramolecular charge transfer (ICT). Compounds **1** and **2** with the unsubstituted carbazole fragment are characterized by slightly higher values of PLQY of THF solutions than derivatives **3** and **4** with the *tert*-butyl substituted carbazole moiety (Table 2.1). Also, it was found that compounds **1** and **2** showed aggregation-caused quenching (ACQ), since the PLQYs of solid samples were found to be lower in comparison to those of the corresponding dilute THF solutions. In contrast, compounds **3** and **4** showed aggregation-induced emission enhancement (the PLQYs of the solid samples were found to be higher than the corresponding PLQYs of the dilute THF solutions). It is likely that the relatively bulky *tert*-butyl groups hinder close stacking of the aromatic moieties as well as intermolecular π-π interactions.

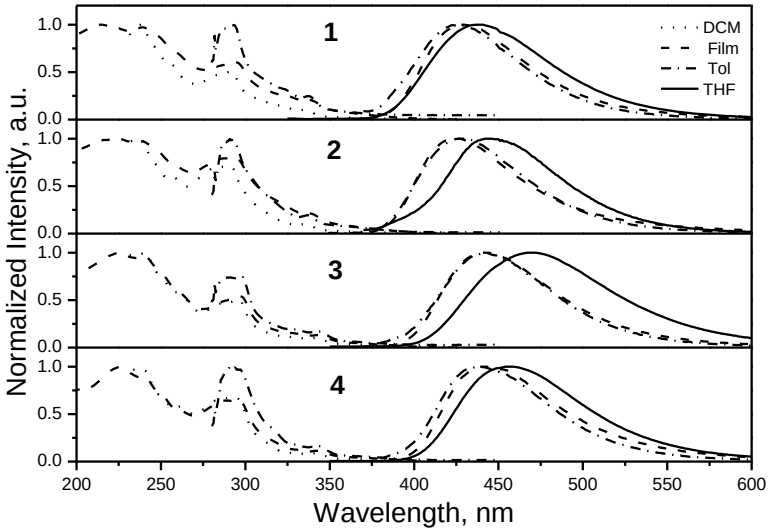

Fig. 2.2. UV and PL (λ_{ex}=330 nm) spectra of dilute solutions and of solid films

The energies of the first singlet (E_S) and triplet (E_T) levels were estimated from the PL and phosphorescence (Ph) spectra of THF solutions at 77K, the values of E_S and E_T were found to be in the range of 3.13–3.33 eV and 2.97–3.04 eV, respectively (Table 2.1). Also, it was found that the attachment of *tert*-butyl substituents resulted in a negligible decrease of the triplet energies of the studied carbazole-oxadiazole based derivatives.

Cyclic voltammetry (CV) measurements of acetonitrile solutions were performed for all the synthesized derivatives (Fig. 2.3a). The ionization potential (IP_{CV}) and the electron affinity (EA_{CV}) values were determined from the onset of oxidation and reduction potentials. The estimated EA_{CV} values of derivatives **1–4** were found to be fairly similar (2.28–2.41 eV), with the IP_{CV} values ranging from 5.46 eV to 5.90 eV (Table 2.2). The ionization potentials (IP_{PE}) of the solid layers of the target compounds were estimated as well (Fig. 2.3b). The IP_{PE} values were taken from the intersection points of the fit lines to the linear parts of the spectra with the abscissa axis (Table 2.2). The electron donating effect of the *tert*-butyl groups resulted in lower IP_{PE} values of compounds **3** and **4** in comparison with the non-substitute analogues

(materials **1** and **2**). Also, the solid-state EA_{PE} was calculated (Table 2.2). It is notable that the energy values of IP and EA obtained by photoelectron spectroscopy and from CV measurements are in good correlation.

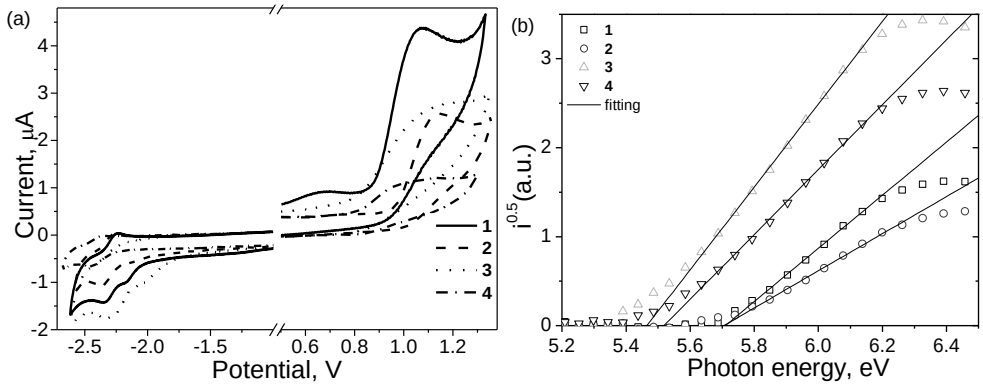

Figure 2.3. CV curves (a) and photoelectron emission spectra (b) of compounds **1–4**

Table 2.2. Electrochemical characteristics of compounds **1**–**4**

Comp.	$E_{ox\ vs\ Fc^+/Fc}^{onset}$	$E_{red\ vs\ Fc^+/Fc}^{onset}$	$IP_{cv.}$, eV	EA_{CV}, eV	E_g, eV	IP_{PE}, eV	EA_{PE}, eV
1	0.92	-2.01	5.88	2.38	3.45	5.71	2.26
2	0.93	-2.10	5.90	2.28	3.43	5.71	2.28
3	0.76	-2.09	5.66	2.29	3.44	5.46	2.02
4	0.62	-1.99	5.46	2.41	3.42	5.52	2.10

$E_{ox\ vs\ Fc^+/Fc}^{onset}$, $E_{red\ vs\ Fc^+/Fc}^{onset}$ – onsets of oxidation and reduction potentials respectively; IP – the ionization potential, $IP_{CV} = -1.4 * E_{ox}^{onset} - 4.60$; EA – electron affinity, $EA_{CV} = -1.19 * E_{red}^{onset} - 4.78$; E_g – optical band gap from the onset of the absorption spectra of thin films; IP_{PE} and EA_{PE} – the ionization potentials and electron affinity of solid state films, respectively; $EA_{PE} = IP_{PE} - E_g$

One of the valuable properties of organic electroactive materials for the potential application in OLEDs fabrication is the balanced charge transport of positive and negative charges. Thus, the charge-transporting properties of compounds **1–4** were measured with the time-of-flight (TOF) technique, and the electric field dependencies of hole end electron drift mobilities of the vacuum deposited layers of derivatives **1–4** are illustrated in Fig. 2.4. From the obtained results, it was found that all the synthesized derivatives are able to transport electrons, while derivatives **2** and **3** are characterized by bipolar charge-transport properties. Moreover, for compounds **1** and **4**, the charge mobilities of electron transport were lower by ca. one order of magnitude than for compounds **2** and **3**. The differences in the hole and electron mobilities of compounds **1–4** can be explained by the different intermolecular interactions between molecules in solid state films. Also, different spatial frontier orbital distributions[45] and geometries of the molecular structures[46] result in distinctions pertaining to charge-transporting properties. In addition, compound **2** is characterized by comparable hole and electron mobilities across the full range of the applied electric field. The highest value of charge mobilities was found to be 10^{-4} cm^2/Vs for both electrons and holes at a moderate electric field. The bipolar

charge transport for compound **3** was confirmed by photo-CELIV (Fig. 2.4). The obtained mobility values were found to be in good agreement with those obtained by TOF.

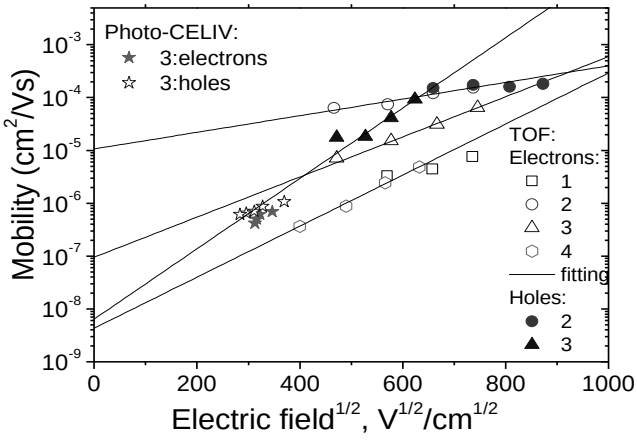

Fig. 2.4. Electric field dependencies of charge mobilities for the layers of compounds **1**–**4**

Considering the high values of triplet energy levels (up to 3.04 eV) and bipolar charge mobilities, the synthesized compounds were used as host materials together with bis(4',6'-difluorophenylpyridinato)-iridium (III) picolinate (FIrpic) as the emitter with a high triplet energy level value of 2.70 eV for the fabrication of blue phosphorescent devices. Several electroluminescent (EL) devices with structures ITO/MoO_3(2nm)/ TCTA(40nm)/mCP(8nm)/ tested host (**1**–**4,** and mCP):Flrpic (*ca.* 7 wt%) (32nm) /TSPO1(8nm) /TPBi(40nm)/Ca/Al were fabricated (Fig. 2.5a).

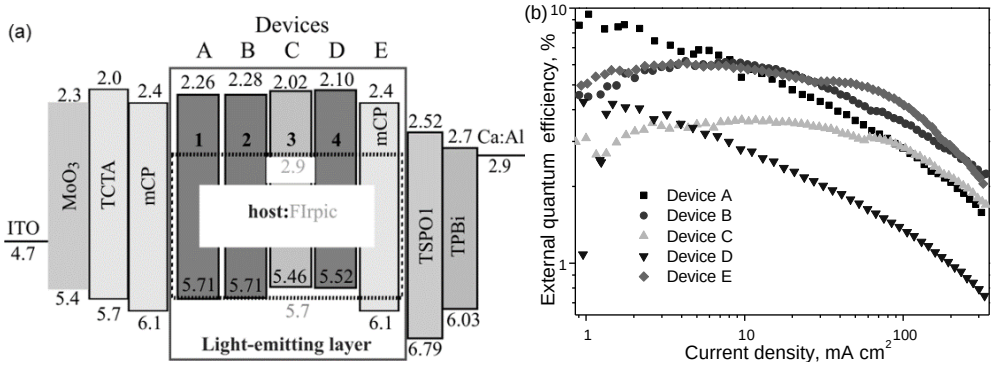

Fig. 2.5. Equilibrium energy diagram (a) and current/external quantum efficiencies versus current density plots (b) for devices A–E based on hosts **1**–**4**

All the fabricated devices are characterized by similar EL spectra at applied different voltages exhibiting an emission band of FIrpic. The turn on voltages were found to be in the range of 4.3 V–6.2 V with 5000 cd/m^2 of maximum brightness of the constructed devices. The maximum external quantum efficiencies (EQE) of devices A–E ranged from 3.6% to 8.8% (Fig. 2.5b). The highest values of EQE were found for devices based on oxadiazole derivatives with non-substituted carbazole

moieties (hosts **1** and **2**), while the lower values of EQE were observed for host materials **3** and **4** containing a *tert*-butyl-substituted carbazole moiety. Also, the similarities of EQE values of devices A, B and E based on host materials **1**, **2** and mCP, respectively, with the same OLED structure were observed. The different values of device efficiencies with quite similar structures, except for the used hosts, can be explained by the diverse charge injection efficiency at the interfaces between the charge-transporting and the light-emitting layers, as well as by the differences in the charge-transporting properties of the hosts and in the energy transfer efficiency between the hosts and the emitter. The maximum values of EQE of 8.8% and of brightness of 8700 cd/m^2 at applied voltage of 10 V were found for the best fabricated device A based on host material **1** featuring pure emission of the phosphorescent emitter.

2.2. Polymorphism of *tert*-butyl substituted acridan and perfluorobiphenyl moiety: synthesis and investigation (Scientific publication No. 2, Q1, 15 quotations)

This chapter is based on the paper published in *J. Mater. Chem. C*, **2018**, *6*, 1317 –13189[47]. Novel blue emitting multi-functional luminophores showing the TADF, AIEE and blue ↔ sky-blue color changing property were synthesized and characterized. Perfluorobiphenyl (PFBP) was used as the acceptor for the first time. 9,9-dimethylacridan (DMAC) was chosen due to its strong donor ability. Also, in order to obtain materials with improved thermal, morphological and electrochemical stabilities, 2,7-di-*tert*-butyl-9,9-dimethylacridan was used. The chemical structures and the synthetic pathway of four new D-A/D-A-D PFBP derivatives are presented in Scheme 2.2. The target materials are well soluble in polar solvents: DCM, THF, acetonitrile, and acetone. The chemical structures of the synthesized compounds were characterized by ^{1}H, ^{13}C and ^{19}F NMR spectroscopy, X-ray single crystal analysis, and ESI-MS mass spectrometry.

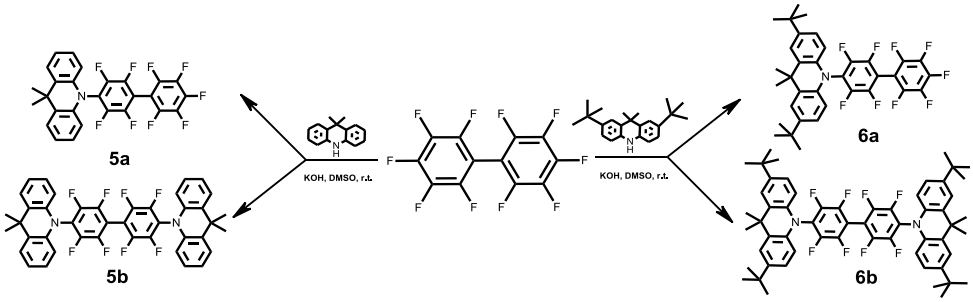

Scheme 2.2. Synthesis of acridan-substituted perfluorobiphenyl derivatives

Theoretical calculations of the PFBP derivatives were performed, and the geometries of the molecular structures were optimized at B3LYP functional level with 6–31+G* basis set in vacuum. The HOMO and LUMO orbital distributions and their energy values are presented in Fig. 2.6. The energy values of the HOMO and LUMO orbitals were found to be in the ranges of -5.3 eV to -5.6 eV and -2.2 eV to -2.3 eV, respectively.

The thermal stability and morphological properties of PFBP derivatives were investigated by TGA and DSC, respectively. The values of T_{ID}, T_m, T_g and the crystallization temperature (T_{cr}) are summarized in Table 2.2. The target compounds with the D-A structure (**5a** and **6a**) were characterized by lower T_{ID} and T_m in comparison with the derivatives featuring the D-A-D structure (**5b** and **6b**), apparently due to the high reactivity of the fluorine atom situated at the C-10' position of the PFBP unit in monosubstituted derivatives. All the synthesized PFBP materials were isolated after the synthesis and purification as crystalline substances. Moreover, two values of T_m were observed for **6a** in the first heating scan (212 ºC and 221 ºC) due to the presence of two different crystal structures of **6a**. It is notable that after cooling and the second heating scan, only T_m at 221 ºC was observed.

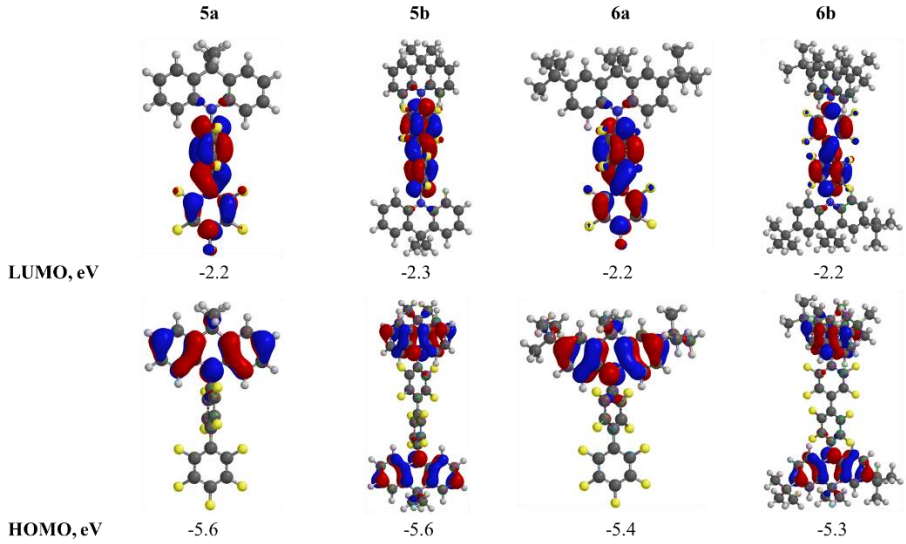

Fig. 2.6. Theoretical calculations for the synthesized PFBP compounds

Table 2.3. Thermal, electrochemical and photoelectrical characteristics of PFBP derivatives

Comp.	T_{ID}[a], °C	T_m[b], °C	T_{cr}, °C	T_g[d], °C	$E_{ox\ vs\ Fc^+/Fc\ onset}$	$E_{red\ vs\ Fc^+/Fc\ onset}$	IP_{CV}, eV	EA_{CV}, eV	IP_{PE}, eV
5a	205	189	121[c, d]	–	0.82	-2.17	5.75	2.19	6.43
5b	303	217	157[d]	98	0.83	-2.08	5.76	2.30	6.19
6a	232	212,221	109[d]	64	0.63	-2.21	5.48	2.15	5.92
6b	317	310	288[c]	–	0.62	-2.06	5.47	2.33	5.88

[a] Determined by TGA. [b] DSC first heating scan. [c] DSC cooling scan. [d] DSC second heating scan. $E_{ox\ vs.\ Fc^+/Fc}^{onset}$, $E_{red\ vs.\ Fc^+/Fc}^{onset}$ – onsets of oxidation and reduction potentials respectively; IP – ionization potential; $IP_{CV} = -1.4 \times E^{onset}{}_{ox} - 4.60$. EA – electron affinity; $EA_{CV} = -1.19 \times E^{onset}\ red - 4.78$. IP_{PE} – ionization potentials of solid films.

CV was used to investigate the redox behavior of PFBP derivatives. CV measurements were done in a dry DMF solution, and the obtained CV curves are

presented in Fig. 2.7a, whereas the calculated IP_{CV} and EA_{CV} values are summarized in Table 2.3. As it was predicted by theoretical calculations, the derivatives containing non-substituted DMAC moieties (**5a** and **5b**) are characterized by slightly higher IP_{CV} values (5.75 eV and 5.76 eV) than the materials substituted by *tert*-butylated DMAC fragments **6a** and **6b** (5.48 eV and 5.47 eV). Also, D-A (**5a** and **6a**) and D-A-D (**5b** and **6b**) type materials are characterized by similar EA_{CV} values (2.19 eV and 2.13 eV, 2.30 eV and 2.33 eV, respectively, Table 2.4). The IP_{PE} of the solid layers of PFBPs were measured as well (Fig. 2.7b). The values of IP_{PE} were found to be higher than the IP values obtained by CV (Table 2.3), probably due to the difference in molecular interactions and arrangements in dilute solutions and in the solid layers of PFBP derivatives. IP_{PE} and IP_{CV} values of **6a** and **6b** were found to be slightly lower than for **5a** and **5b**, which was caused by the electron donating effect of *tert*-butyl groups.

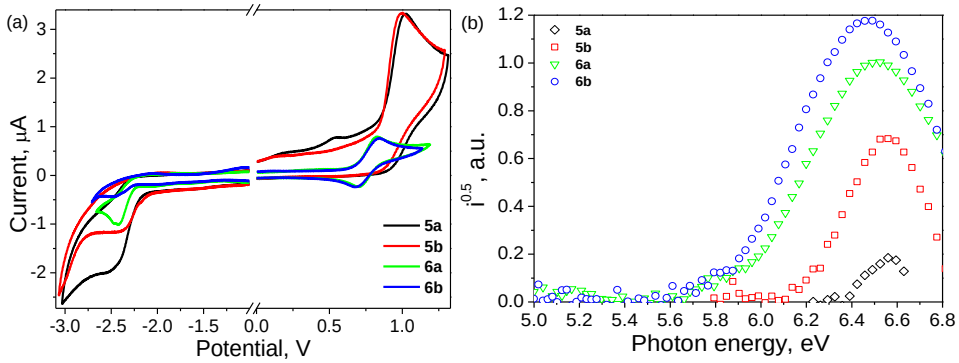

Fig. 2.7. CV curves and photoelectron emission spectra of the synthesized compounds

The UV-Vis and PL spectra of the target PFBP derivatives in different media are depicted in Fig. 2.8a. The wavelengths of absorption and emission maxima are listed in Table 2.4. The absorption bands ranging from 348 nm to 371 nm of toluene and THF solutions are related to the ICT of PFBP derivatives. PFBP derivatives with the *tert*-butyl-substituted DMAC moiety (**6a** and **6b**) are characterized by slight bathochromic shifts of the absorption spectra of solid films correspondingly in their dilute solutions as a result of intermolecular interactions in the solid state.

Table 2.4. Photophysical data of PFBP derivatives

Compound	λ_{abs}[a/b/c], nm	λ_{PL}[a/b/c], nm	Φ_{PL}	Φ_{PL}[c]
5a	348/356/356	531/493/418	0.04[a]	0.27
5b	355/362/362	531/497/482	0.1[a]	0.34
6a	364/371/371	556/528/486[d],463[e]	0.03[b]	0.43[d]/ 0.61[e]
6b	370/364/376	562/516/494	0.08[b]	0.46

[a] THF solution. [b] Toluene solution. [c] Solid state. [d] For vacuum deposited films (amorphous) before treatment with toluene vapor. [e] For vacuum deposited films (crystalline) after treatment with toluene vapor. λ_{abs} is the wavelength of the absorption maximum; λ_{PL} is the wavelength of the PL intensity maximum; Φ is the photoluminescence quantum yield.

A strong solvatochromic effect of PL emission of PFBPs was observed and resulted in bathochromic shifts of the PL spectra in highly polar solvents. Thus, the bathochromic shifts of PFBP derivatives emission in the solution of THF in comparison with the low-polar toluene solution were observed (Fig. 2.8a). The emission in the sky blue region of the solid samples was observed for PFBP derivatives containing the *tert*-butyl substituted DMAC moiety (**6a** and **6b**), whereas compounds having non-substituted DMAC components (**5a** and **5b**) emitted light in the deep-blue and the sky-blue region, respectively (Fig. 2.8a, Table 2.4). The hypsochromic shift of the emission in the solid state was observed for all the PFBP derivatives in comparison with the emission of their THF and toluene solutions (Fig. 2.8a). Moreover, a further hypsochromic shift of the film emission of **6a** was observed after the treatment of toluene vapor (Fig. 2.8b), which is related to the polymorphism of this compound. The vapor of hydrophobic solvent toluene may apparently change the molecular packing of the film because of extracting the hydrophobic parts of the molecules into the surface during evaporation. Thus, the changes in the structure led to transformations in electronic interactions between the molecules in the film and resulted in the hypsochromic shift of the PL spectra. Furthermore, the sky-blue ↔ blue emission color changes of **6a** film (Fig. 2.8c) were observed when applying external stimuli (upon grinding with a spatula and heating at 64–66 ºC for 2–3 minutes), which demonstrated the MCL properties of this compound.

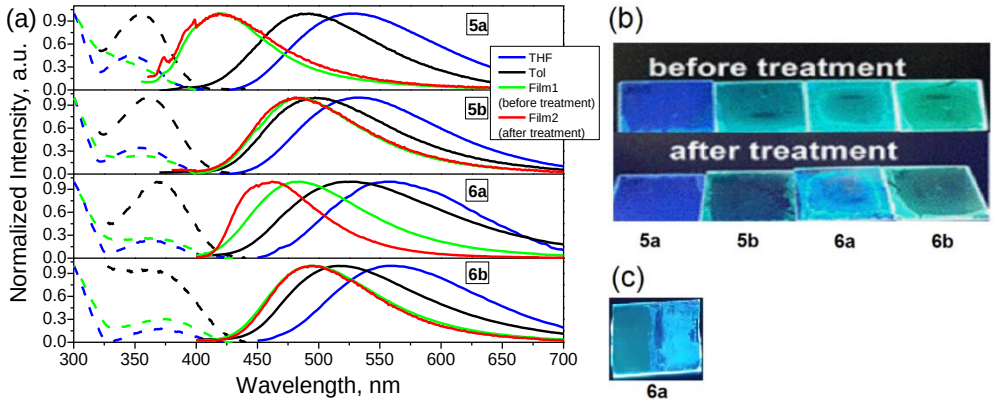

Fig. 2.8. UV (dashed lines) and PL (solid lines) spectra of the solutions of PFBPs, and of the films (a). The color of emission of the films before and after treatment with toluene vapor (b); before (the left side) and after applying external stimuli (the right side) film based on compound **6a** under UV excitation (c)**.**

All the PFBP derivatives are characterized by higher photoluminescence efficiency in the solid state in comparison to their solutions due to the AIEE effect. Moreover, crystalline and amorphous films of compound **6a** are characterized by different PLQY values (0.61 and 0.43, respectively). The AIEE effect was studied by the measurements of PL intensity of THF/water solutions with different ratios of water. The PL spectra of the dispersions of PFBPs in water/THF mixtures are shown in Fig. 2.9.

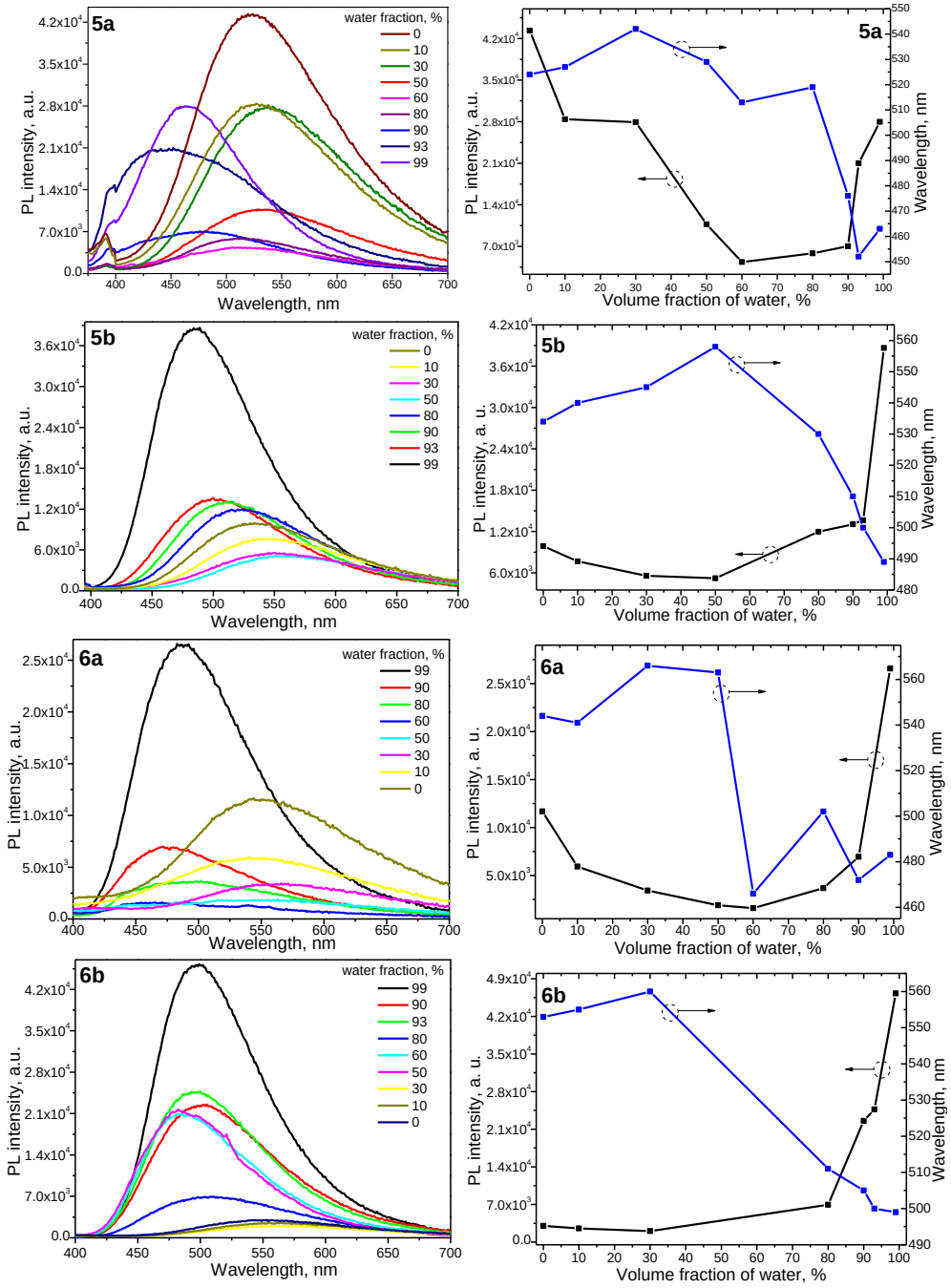

Fig. 2.9. PL profiles of PFBPs in water/THF mixtures with different water fractions

A small bathochromic shift of the PL maximum was observed with the increase of the water fraction up to 40% compared to that of the dilute THF solution due to an increase of the polarity of water/THF mixtures with the increase of the water ratio. However, an increase of the PL intensity and the hypsochromic shift of the PL

maxima of the dispersions were detected at a further increase of the water fraction (f_w) above 40% (Fig. 2.9). The wavelengths of the PL maximum of the dispersion of PFBPs in the water/THF mixture (f_w=99 %) were found to be close to those of the PL maximum of the solid samples of PFBPs. However, a slightly different behavior was observed for compound **5a**. A small bathochromic shift of the PL maximum and a decrease of PL intensity was observed with the increase of the water fraction (f_w) up to 60% compared to that of the dilute THF solution. A hypsochromic shift of the PL maxima and a slight increase of the PL intensity were detected at a further increase of the water fraction above 60%. However, the aggregates of **5a** in the aqueous mixture with f_w of 99% were characterized by lower PL intensity in comparison with the pure THF solution, probably due to the excess of water which may accelerate the aggregation process and influence the regular arrangement of **5a** molecules and may lead to the exhaustion of the electronic excited energy via intramolecular rotations, and less emissive nanoaggregates are formed[48]. The obtained results demonstrate aggregation of PFBPs molecules due to the poor solubility of the obtained derivatives in water and prove the AIEE effect. The TADF effect of the obtained PFBP derivatives was investigated. Transient PL decay curves of solid films were recorded in inert atmosphere at temperatures ranging from 77 K to 300 K (Fig. 2.10).

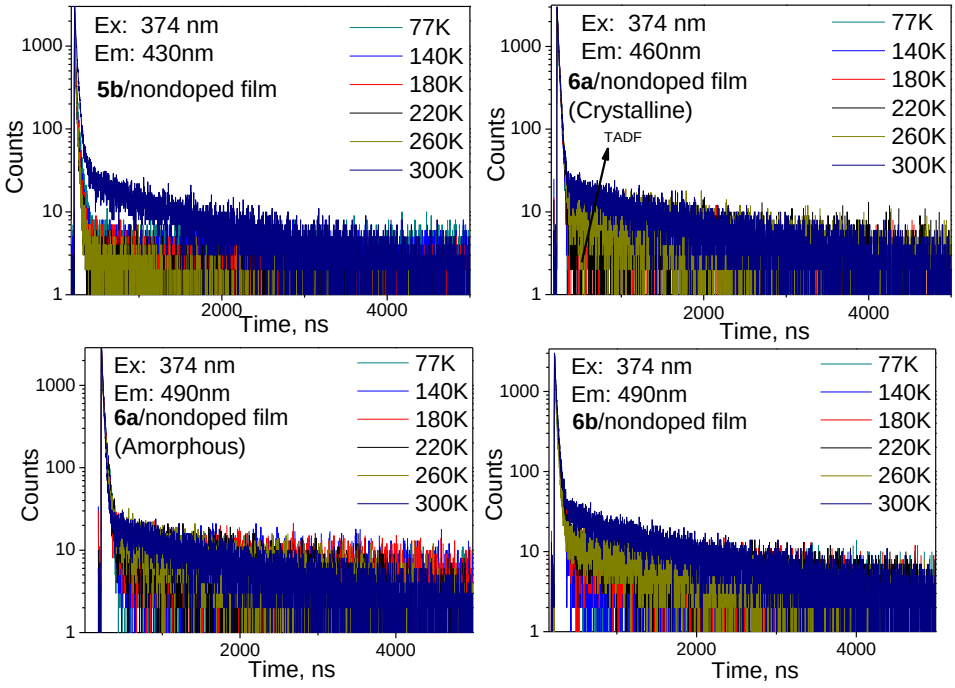

Fig. 2.10. PL decay curves of vacuum deposited layers of **PFBPs** at different temperatures

The PL decay curves of **6a** were measured from treated and non-treated films due to dual emission in the solid state. An increase of the intensity of the delayed component with the increase of temperature was observed for all the PFBP derivatives including both polymorphs of **6a**. The PL and Ph spectra at 77 K of THF solutions and of solid films were recoded as well. Negligible differences between the singlet

and the triplet state ($\Delta E_{S\text{-}T}$) was observed for all the derivatives due to very similar PL and Ph spectra of the solutions in THF and solid films.

Measurements of the charge-transporting properties of PFBP materials by the TOF technique were performed, but, due to very dispersive charge transport, it was extremely difficult to take the transit times for the studied samples at different applied electric fields for holes and electrons from the corresponding photocurrent transients for all the tested samples. Only for **6b**, the transit time was exactly defined. The hole mobility of ca. 1.0×10^{-4} cm^2/Vs at an electric field of 6×10^5 V/cm for **6b** was determined.

Two polymorphs of **6a**, which were named crystal A and crystal B (Fig. 2.11a, b), were obtained, and their crystal structures were investigated by single crystal X-ray diffraction analysis. **6a**_crystal A crystallizes in the monoclinic space group $P2_1/c$, while polymorph **6a**_crystal B crystallizes in the triclinic space group $P\bar{1}$.

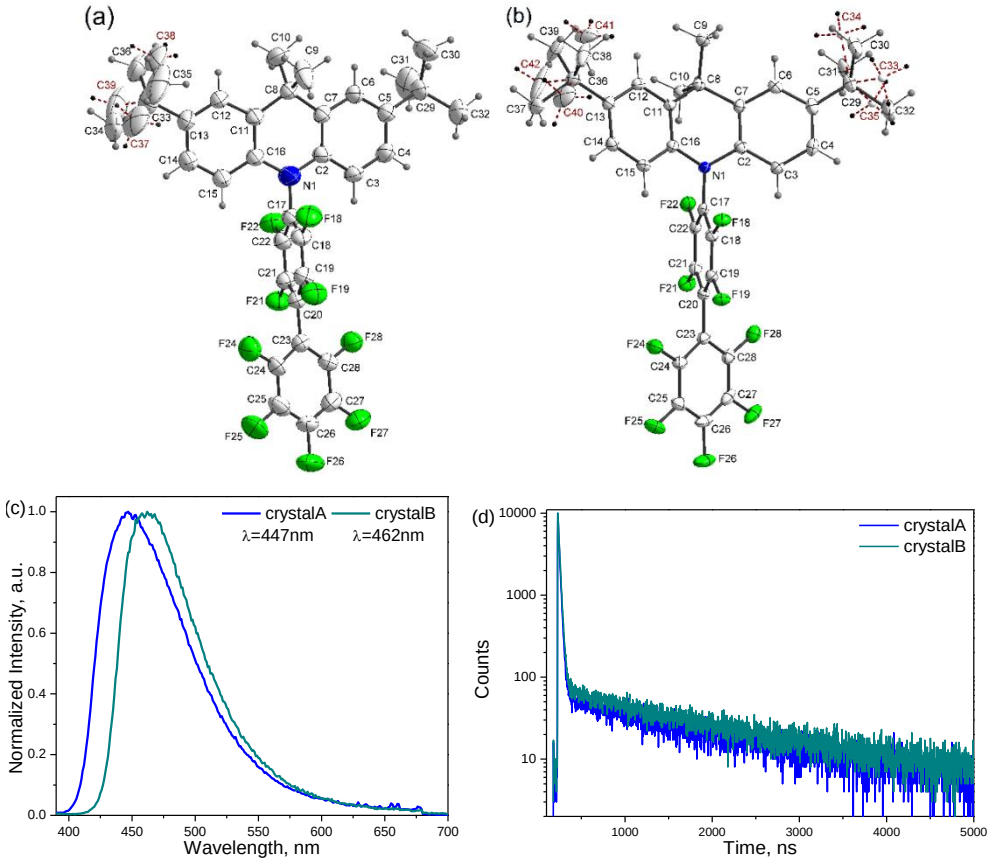

Fig. 2.11. The atom-numbering scheme of the asymmetric units of **6a**_crystal A (a) and **6a**_crystal B (b), PL spectra (c) and decay curves (d) of **6a**_crystal A and **6a**_crystal B

According to the X-ray analysis, the main difference between the crystal structures of **6a**_crystal A and **6a**_crystal B is the structural deformation of the position of methyl groups in position 9 of *t*-Bu-DMAC in crystal **6a**_crystal B. The

distance between the corresponding hydrogen atom and the closest fluorine atom in **6a**_crystal B is significantly lower (2.814 Å) comparing to the respective C-H···F length in **6a**_crystal A (4.104 Å). When comparing these distances to the sum of Van der Waals radii of Fluorine and Hydrogen atoms (2.67 Å), the measured C-H···F distance in **6a**_crystal B is found to feature a very close value to the minimal one required for the formation of the hydrogen bond (Fig. 2.11b). Taking into account the differences between the physical properties of the investigated substances, we can conclude that this bond is apparently formed and exerts influence on the photophysical and thermal properties, while the small distance difference between the C-H···F length in **6a**_crystal B and the sum of Van der Waals radii is apparently suppressed by molecular vibrations allowing to form a weak C-H···F hydrogen bond in **6a**_crystal B. Also, the PL spectra and excited-state lifetimes of crystals **6a**_crystal A and **6a**_crystal B were measured (Fig. 2.11c, d). The obtained results are in good agreement with those measured from films.

Several OLEDs based on novel TADF emitters (**5b**, **6a** and **6b**) with the following structures: ITO/ MoO_3/NPB/emitters (**5b**:mCP, **6a**:TCz1 or **6b**:TCz1/TPBi/Ca:Al were manufactured (Fig. 2.12a). Also, compound **6b**, due to its highest PLQY in the solid state, was used for the construction of a non-doped device with the structure ITO/MoO3/NPB/**6b**/TPBi/Ca/Al.

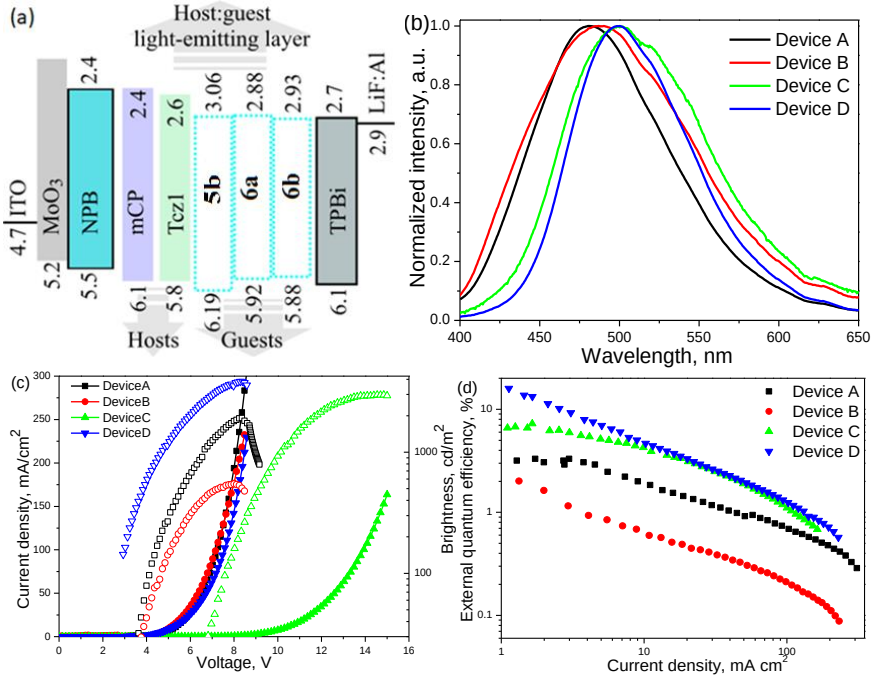

Fig. 2.12. Equilibrium energy level diagrams (a), EL spectra (b) current density/brightness versus voltage plots (c) and current/external quantum efficiencies versus current density plots (d) for devices A–D

The maxima of the EL spectra of the manufactured devices A, B, C and D are generally located in the sky-blue and greenish-blue regions (Fig. 2.12b) with the

intensity maxima at 480 nm, 488 nm, 499 nm and 499 nm, respectively, and are listed in Table. 2.5. The chromaticity coordinates of the devices according to *Commission Internationale de l'Eclairage* (CIE 1931) are presented in Table 2.5. The values of turn-on voltage for the doped devices (A, B and D) were found to be much lower (3.8 V, 3.9 V and 3.0 V, respectively) than for non-doped device C (7.0 eV). The high turn-on voltage of device C is achieved due to the strongly dispersive charge transport of non-doped film **6b**. The best fabricated device D achieved the maximum values of EQE of 16.3%, the current efficiency (CE) of 30.8 Cd/A, and the power efficiency (PE) of 22.7 lm/W (Table 2.5). Negligible singlet-triplet energy splitting (0.06 eV), high PLQY (73%) of the molecular mixture **6b**:TCz1, and the ambipolar charge-transporting properties of the host TCz1[49] resulted in high EQE owing to the efficient exciton up-conversion from non-emissive triplets to emissive singlets in this device.

Table 2.5. OLEDs characteristics

Device	V_{on}, V	Max. brightness, Cd/m^2	η_c^{max}, Cd/A	η_p^{max}, lm/W	EQE^{max}, %	λ_{max}^{EL},nm	CIE, (x, y)
A	3.8	1850	6.5	4.4	3.3	480*	(0.177, 0.266)*
B	3.9	550	3.7	2.5	3.9	487*	(0.199, 0.289)*
C	7.0	3000	16.3	5.8	6.6	499**	(0.222, 0.388)**
D	3.0	3900	30.8	22.7	16.3	499*	(0.202, 0.419)*

* at 6V. ** at 12 V. Device structures: A – ITO/MoO_3/NPB/**5b**:mCP/TPBi/Ca/Al; B – ITO/MoO_3/NPB/**6a**:TCz1/TPBi/Ca/Al; C – ITO/MoO_3/NPB/**6b**/TPBi/Ca/Al; D – ITO/MoO_3/NPB/**6b**:TCz1/TPBi/Ca/Al.

2.3. Investigation of photophysical properties of organoboron complexes (benzo[4,5]-thiazolo[3,2-*c*][1,3,5,2]oxadiazaborinines) (Scientific publications No. 3 and No. 4. Scientific publication No. 3, Q1, 4 quotations, scientific publication No. 4, Q1)

This chapter is based on the papers published in *J. Org. Chem.*, **2018**, *83*, 12129−12142[50] and *J. Org. Chem.*, **2019**, *84*, 5614−5626[51]. Organoboron complexes are promising candidates for potential application in OLEDs and as a laser dye for a cholesteric liquid crystal laser[52], OPVs[53], as the photoactive element in organic solar cells[54], etc., due to good photophysical properties (e.g., high PLQY, a relatively long lifetime of the excited state, high solubility in organic solvents[55]). The two groups of materials based on benzo[4,5]thiazolo[3,2-*c*][1,3,5,2]-oxadiazaborinines (Fig. 2.13) moieties were designed and synthesized by dr. M.A. Potopnyk. Their photophysical and electrochemical properties were investigated.

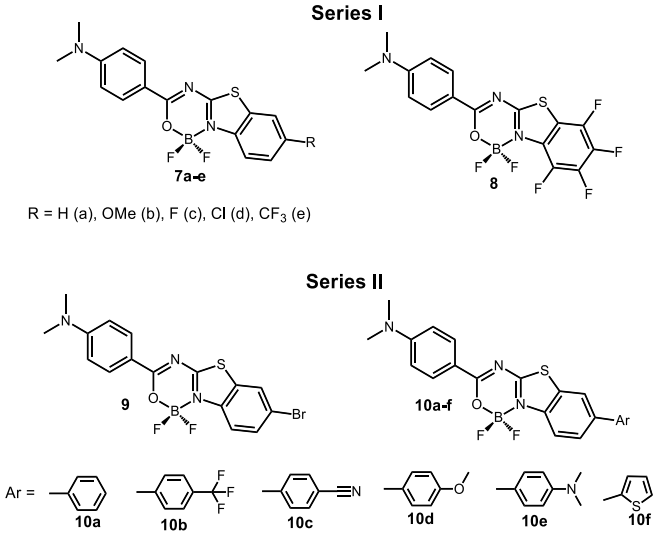

Fig. 2.13. Chemical structures of the studied organoboron complexes

The absorption and PL spectra of dilute solutions and of solid films of compounds **7a–e** and **8** of Series I and of compounds **9** and **10a–f** of Series II are presented in Fig. 2.14a and b, respectively. The maxima values of absorption and emission wavelengths are collected in Table 2.6. The studied derivatives (**7a–e** and **8**) are characterized by a single absorption peak in solutions and located in the region of 411–434 nm related to the $S_0 \rightarrow S_1$ transition. The studied materials (**9** and **10a–f**) are characterized by a single absorption peak in the violet-blue region, and the wavelength maxima of the solutions are located in the region of 427–439 nm.

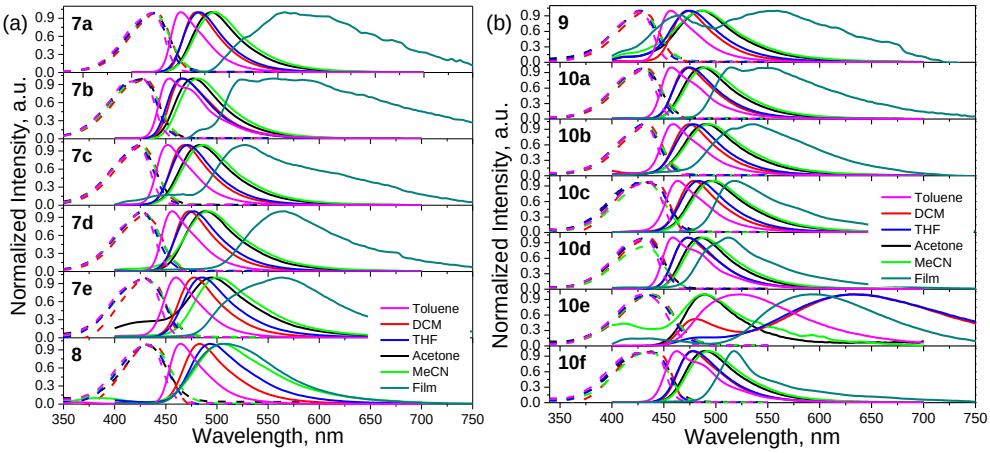

Fig. 2.14. Absorption (dashed lines) and emission (solid lines) spectra of the solutions and of solid states of complexes **7a–e**, **8** (a) and **9**, **10a–f** (b)

All organoboron dyes of Series I demonstrated positive solvatochromism. While increasing the solvent polarity from toluene to acetonitrile, a bathochromic shift of the emission maxima was observed (450 → 486 nm for **7a**, 454 → 481 nm for **7b**,

452 → 487 nm for **7c**, 456 → 491 nm for **7d**, 460 → 500 nm for **7e**, 464 → 503 nm for **8** (Fig. 2.14a). The influence of the electronic structure of the benzothiazole residue on the photophysical properties was observed by the comparison of the emission spectra of organoboron complexes **7a–e** and **8** (Fig. 2.14). The attachment of stronger electron-accepting units to the benzothiazole moiety resulted in more bathochromic shifts of the emission bands for the solutions in all the solvents (λ_{PL} (**8**) > λ_{PL} (**7e**) > λ_{PL} (**7d**) > λ_{PL} (**7c**) > λ_{PL} (**7a**), Table 2.6).

Table 2.6. Photophysical data of compounds **7a–e, 8, 9, 10a–f**

Comp.	λ_{abs} [a/b/c/d/e], nm	λ_{PL} [a/b/c/d/e/f], nm	Φ_{PL} [a/b/c/d/e/f]
7a	421/425/421/425/424	450/467/469/482/468/557	0.84/0.77/0.78/0.31/0.17/0.03
7b	411,427/430/426/431/430	454/467/466/477/481/555	0.88/0.83/0.80/0.56/0.38/0.05
7c	423/425/422/426/425	452/468/472/483/487/528	0.85/0.74/0.72/0.23/0.13/0.02
7d	427/430/426/430/430	456/473/477/488/491/566	0.91/0.78/0.74/0.21/0.12/0.02
7e	428/431/427/431/430	460/478/486/495/500/563	0.93/1/0.61/0.13/0.05/0.03
8	431/433/431/432/434	464/483/492/463/503/506	0.65/0.66/0.47/0.06/0.02/0.34
9	427/431/430/427/426	450/467/469/482/486/464,559	0.74/0.61/0.55/0.27/0.13/0.03
10a	430/432/430/430/430	457/473/475/487/491/515	0.92/0.74/0.82/0.56/0.33/0.17
10b	431/434/430/430/430	459/475/479/490/493/536	0.80/0.74/0.75/0.42/0.29/0.07
10c	434/436/432/432/431	459/475/479/490/493/518	0.99/0.98/0.96/0.55/0.32/0.31
10d	431/437/431/432/431	459/473/474/485/488/536	0.95/0.79/0.82/0.65/0.43/0.06
10e	430/438/435/436/433	523/480,631/487,630/490/487/667	0.78/0.04/0.03/0.01/0.02/0.12
10f	436/439/435/435/436	462/477/478/489/493/518	0.84/0.91/0.87/0.65/0.44/0.13

[a] Toluene solution. [b] DCM solution. [c] THF solution. [d] Acetone solution. [e] Acetonitrile solution. [f] Solid state. λ_{abs} is the wavelength of the absorption maximum; λ_{PL} is the wavelength of the PL intensity maximum; Φ is the photoluminescence quantum yield.

A slightly different behavior was observed for derivative **7b** containing the electron-donating group OMe. In comparison with compound **7a**, changing of the wavelengths of the emission maxima depends on the solvent polarity (λ_{PL} (**7a**) < λ_{PL} (**7b**) in toluene, (λ_{PL} (**7a**) = λ_{PL} (**7b**) in DCM, λ_{PL} (**6a**) > λ_{PL} (**6b**) in THF, acetone and acetonitrile). The PL spectra of the solid samples of **7a–e** and **8** were found to be bathochromically shifted in comparison to the solutions (Fig. 2.14a). PLQYs values of the solutions in toluene were found to be high for compounds **7a−e** (0.84−0.93), while a lower PL efficiency was found for material **8** (0.65). The PLQY of solid films of compounds **7a–e** was found to be very low (0.02–0.06), while a relatively high Φ_{PL} (0.34) was found for material **8**, which is caused by specific intermolecular interaction in the molecular packing. An increase of the solvent polarity resulted in a lower value of PLQY of all the investigated organoboron complexes (Table 2.6). The photoluminescence efficiencies of the solutions in acetonitrile were found to be very low for dyes **7e** and **8** containing strong electron-withdrawing moieties at the benzo[*d*]thiazole unit (0.05 and 0.02, respectively), while a decrease of the electron-withdrawing strength on the benzothiazole part resulted in slightly higher values of

PLQY (0.12, 0.13 and 0.17 for **7d**, **7c** and **7a**, accordingly). Moreover, complex **7b**, which features an electron-donating group at the benzothiazole moiety, is characterized by the lower impact of the solvent polarity on PL efficiency (0.83, 0.80, 0.56 and 0.38 in DCM, THF, acetone and acetonitrile, respectively). Thus, the ICT character increased with the incorporation of electron-accepting groups into the benzothiazole moiety (**7a** < **7c** < **7d** < **7e** < **8**) and was less prominently expressed for compound **6b** containing the electron-donating group. Also, the lifetimes of the excited state (τ) of the solutions in toluene and of thin films were measured, and the obtained results are listed in Table. 2.7.

All the derivatives of Series II, except for **10e**, are characterized by a single emission band in dilute solutions and demonstrated positive solvatochromism. With increasing the solvent polarity from toluene to acetonitrile, a bathochromic shift of the emission maxima was observed (450 → 486 nm for **9**, 457 → 491 nm for **10a**, 459 → 493 nm for **10b**, 459 → 493 nm for **10c**, 459 → 488 nm for **10d**, 462 → 493 nm for **10f** (Fig. 2.14b). A totally different behavior was observed for compound **10e**. It was found that the intensities of the high-energy and low-energy emission bands of **10e** are highly dependent on the polarity of the solvents. Thus, acetone and acetonitrile solutions of **10e** exhibit blue-shifted peaks located at 487−490 nm; diluted solutions of DCM and THF of organoboron complex **10e are** characterized by a dual emission band with the emission peaks maxima around 480−487 nm and 630 nm, appropriately; an intensity maximum at 523 nm was observed in its toluene solution.

In order to investigate the nature of the dual emission in the high- and low-energy regions of compound **10e**, the Lippert−Mataga equation was used. The Stokes shifts (ν_{abs}-ν_{em}) versus the orientation polarizability of solvents (Δf) dependencies were plotted and linearly fitted (Fig. 2.15). The low (1938 cm^{-1}) and high (14694 cm^{-1}) slope values were observed in the high- and low-energy regions, respectively. The single emission bands in the high- and low-energy regions were observed for the solution in solvents with relatively high (acetone and acetonitrile) and low (toluene and chloroform) orientation polarizability (Δf), correspondingly. Moreover, a dual emission with bands in both high- and low-energy regions were observed for the solutions of complex **10e** dissolved in solvents with average Δf (THF, DCM, Et_2O). The cause of this effect could be related to the ICT nature which is sensitive to solvent polarity. The high energy band of the emission of complex **10e** is related to ICT due to donating the (N,N-dimethylamino)phenyl group attached directly to the 1,3,5,2-oxadiazaborinine ring to the accepting benzo[4,5]thiazolo[3,2-*c*][1,3,5,2]-oxadiazaborinine moiety, similarly to the emission of complexes **9** and **10a−d**,**f** (Fig. 2.14b), while the low-energy emission band of dye **10e** is probably related to ICT from the (N,N-dimethylamino)phenyl donor substituent at position 6 of the benzo[*d*]thiazole unit to the benzo[4,5]thiazolo[3,2-*c*][1,3,5,2]oxadiazaborinine acceptor. Thus, the emission of compound **10e** is probably caused by both ICT emissive excited states.

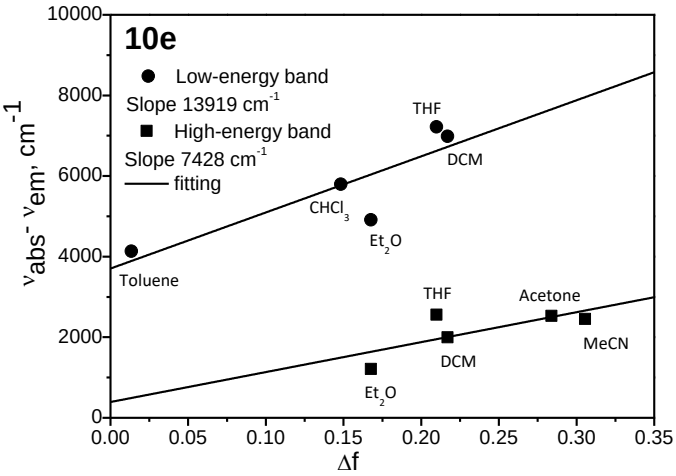

Fig. 2.15. Lippert–Mataga plot of the solutions of complex **10e**

Table 2.7. Photophysical and electrochemical characteristics of compounds **7a–e, 8, 9, 10a–f**

Comp.	τ, ns[a/b]	χ^2, [a/b]	$E_{ox\ vs\ Fc^+/Fc}^{onset}$	$E_{red\ vs\ Fc^+/Fc}^{onset}$	IP_{CV}, eV	EA_{CV}, eV
7a	1.74/0.81;4.10	1.017/1.001	0.72	-2.00	5.12	2.40
7b	1.59/0.88;4.36	1.190/1.015	0.72	-1.99	5.12	2.41
7c	1.68/0.66;3.38	1.177/1.008	0.73	-1.95	5.13	2.45
7d	1.71/1.04;5.90	1.049/1.015	0.73	-1.92	5.13	2.48
7e	1.78/0.99;2.64	1.003/1.148	0.76	-1.83	5.16	2.57
8	2.00/1.77;7.56	1.017/1.002	0.78	-1.65	5.18	2.75
9	1.61/0.65;3.28	1.009/1.018	0.71	-1.90	5.11	2.50
10a	1.43/1.11;4.51	1.099/1.053	0.71	-1.94	5.11	2.46
10b	1.41/1.04;3.87	1.142/1.029	0.70	-1.91	5.10	2.49
10c	1.45/1.12;4.01	1.008/1.003	0.73	-1.88	5.13	2.52
10d	1.39/0.34;2.26	1.018/1.014	0.70	-2.03	5.10	2.37
10e	1.96/0.61;3.86	1.114/1.164	0.24	-1.95	4.64	2.45
10f	1.31/0.69;1.71	1.024/1.272	0.44/0.60	-1.52	4.84/5.00	2.88

τ – excited state lifetime. χ^2 values indicate the accuracy of the experiment. [a] Toluene solution. [b] Solid state. $E_{ox\ vs.\ Fc^+/Fc}^{onset}$, $E_{red\ vs.\ Fc^+/Fc}^{onset}$ – onsets of oxidation and reduction potentials, respectively; IP – the ionization potential; $IP_{CV} = E^{onset}_{ox} + 4.40$. EA – electron affinity; $EA_{CV} = E^{onset}_{red} + 4.40$.

The fluorescence spectra of neat films of organoboron complexes **9** and **10a–f** were found to be bathochromically shifted in comparison with the corresponding dilute solutions (Fig. 2.14b). The PL efficiency of the dilute solutions and the neat film of complexes **9** and **10a–f** were studied, and the corresponding values of Φ_{PL} were collected in Table 2.6. All the studied derivatives exhibited high values of PLQY (0.74–0.99) in toluene solutions, while an increase in the solvent polarity resulted in

a decrease of PL efficiency (Table 2.6). Complete quenching of PLQY in all the solvents (0.01–0.04), except for toluene, for material **10e** was observed and was caused by a high ICT effect. In contrast with toluene solutions, weak fluorescence QY in the solid state (0.03–0.17) of the investigated complexes **9**, **10a, b, d–f** was observed and is probably related to the ACQ effect due to the dense molecular packing. Moreover, a relatively high value of PL efficiency (0.31) in the solid state for **10c** was observed. The cause of this effect can apparently be explained by a decrease of ACQ caused by the specificity of the molecular packing of this compound. The τ of the solutions in toluene and of the solid films of complexes **9** and **10a−f** were measured, and the obtained results are collected in Table 2.7.

The electrochemical properties of the solutions of the studied complexes in dichloromethane solutions were investigated, and the obtained CV curves of Series I and Series II are presented in Fig. 2.15a and b, respectively. The IP_{CV} and EA_{CV} values are summarized in Table 2.7. The IP_{CV} and EA_{CV} values of compounds **7a–e** and **8** were found to be in the region of 5.12 eV – 5.18 eV and 2.40 eV – 2.75 eV, respectively. The IP_{CV} values of compounds **9** and **10a−d** were found to be comparable (5.10–5.13 eV), while derivatives **10e** and **10f** are characterized by significantly lower values of IP_{CV} (4.64 eV and 4.84/5.00 eV), respectively. The calculated EA_{CV} values of **9** and **10a−e** range from 2.37 eV to 2.52 eV, while a considerably higher value of 2.88 eV was found for **10f**.

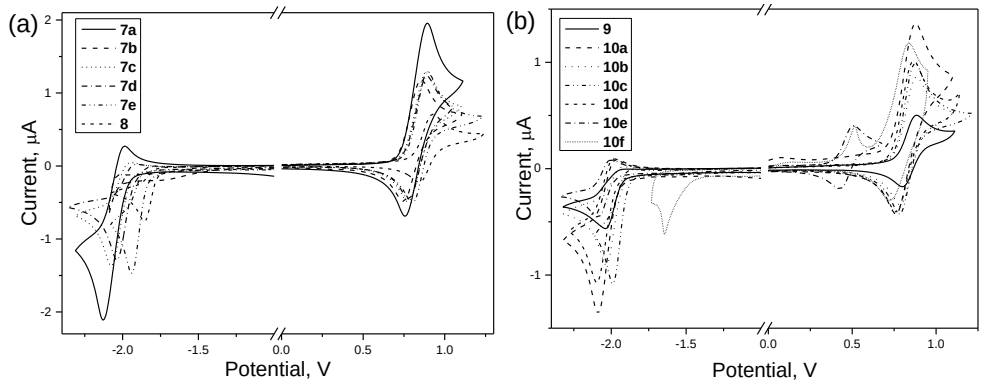

Fig. 2.16. CV curves of complexes **7a–e**, **8** (a) and **9, 10a–f** (b)

In addition, due to the strong crystallization ability of the researched organoboron complexes, it was not possible to obtain samples with a sufficient quality of films for TOF measurements.

3. CONCLUSIONS

1. A series of blue-emitting W-shaped derivatives of carbazole and oxadiazole with the differently substituted phenyl ring were synthesized and characterized as hosts for OLEDs. *Tert*-butyl groups were attached to the carbazole moiety for the improvement of the thermal stability of the compounds and for the morphological stability of their films. It was determined that:

1.1. Derivatives containing the *tert*-butyl substituted carbazole moiety demonstrated a higher temperature of 5% weight loss and glass transition temperature (up to 383 °C and 147 °C, respectively).

1.2. The compounds exhibited a high energy of triplet levels (2.97–3.04 eV). The attachment of electron-donating *tert*-butyl substituents did not significantly affect the energy of the triplet state.

1.3. The layers of the compounds were found to be capable of transporting electrons. Two of them demonstrated bipolar charge-transporting properties with well-balanced hole and electron mobilities reaching 1×10^{-4} cm^2/V at high electric fields.

1.4. The derivatives were suitable for utilization as hosts in blue phosphorescent OLEDs. The best fabricated device demonstrated pure emission of the phosphorescent emitter and reached an 8.8% value of external quantum efficiency and a brightness of 8700 cd/m^2 at the applied voltage of 10 V.

2. Four new donor-acceptor and donor-acceptor-donor derivatives containing perfluorobiphenyl and acridan moieties were synthesized and characterized as blue/sky-blue TADF emitters for OLEDs. It was determined that:

2.1. The compounds were characterized by moderate thermal stability with 5% weight loss temperature exceeding 317 °C; two compounds demonstrated ability to form molecular glasses with glass transition temperatures of 64 and 98 °C. The compounds with the donor-acceptor-donor molecular structure showed a higher 5% weight loss, melting and crystallization temperatures in comparison to their analogues with the donor-acceptor structure.

2.2. The compounds showed blue and sky-blue emission in the solid state with the wavelengths of the emission intensity maxima ranging from 418 to 494 nm. The bathochromic shifts of the emission and higher photoluminescence efficiencies were observed for the compounds with extended π-conjugation (donor-acceptor-donor structure) and additional electron-donating *tert*-butyl groups.

2.3 A photoluminescence quantum yield of 73% was observed for the film of the molecular mixture of one synthesized compound with a high-triplet-energy host. Perfluorobiphenyl derivatives showed a combination of thermally activated delayed fluorescence and aggregation-induced emission enhancement.

2.4. One of the obtained compounds formed two crystalline polymorphs which were characterized by a different color of the emission, with the color changing under external stimuli; the photoluminescence quantum yields of their films were found to be 43% and 61%.

2.5. Perfluorobiphenyl derivatives were found to be suitable for utilization as blue/sky-blue TADF emitters for OLEDs. The best fabricated electroluminescent device showed a low turn-on voltage of 3 V, and the maximum current, power, and external quantum efficiencies of 22.7 cd/A, 30.8 lm/W, and 16.3%, respectively.

3. The photophysical and electrochemical properties of two series of organoboron complexes were investigated. It was determined that:

3.1. The first series of the investigated organoboron complexes demonstrated positive solvatochromism. The photoluminescence quantum yields of the solutions in nonpolar solvents were found to be as high as 65−100%. One of the organoboron complexes was characterized by a moderate quantum yield (34%) in the solid state. The ionization potentials and electron affinities estimated by cyclic voltammetry ranged from 5.12 eV to 5.18 eV and from 2.40 eV to 2.75 eV, respectively.

3.2. The solutions of the studied materials with a functionalized benzo[*d*]thiazole moiety in different solvents were characterized by single emission bands; photoluminescence quantum yields of the solutions of organoboron complexes in non-polar solvents were found to be as high as 78−99%. The solutions of one of the studied derivatives in polar solvents were characterized by dual emission. The ionization potentials and electron affinities estimated by cyclic voltammetry ranged from 4.64 eV to 5.13 eV and from 2.37 eV to 2.88 eV, respectively.

4. SANTRAUKA

4.1. ĮVADAS

Per pastaruosius du dešimtmečius padidėjo organinių puslaidininkių panaudojimas gaminant organinius šviesos diodus (toliau – OLED) ir organinius hibridinius saulės elementus[3]. OLED technologija, ją komercializavus 1997 m., tapo ypač paklausi dėl potencialiai plataus OLED pritaikymo kompiuterių, išmaniųjų telefonų, nešiojamųjų elektronikos prietaisų ir televizorių ekranuose bei apšvietimo sistemose[4]. Dėl unikalių savybių, tokių kaip mažos gamybos sąnaudos, ekranų plonumas, lankstumas, didelis kontrasto santykis, platus stebėjimo kampas ir spalvų gama bei kt., OLED tapo nepakeičiamu prietaisu elektronikos pramonėje. Organinius metalo kompleksus, kurių sudėtyje yra pereinamųjų metalų, turintys fosforescuojantys OLED (toliau – PhOLED) yra plačiai naudojami, kadangi dėl susidarančių singletinių-tripletinių eksitonų panaudojimo jie gali pasiekti iki 100% vidinį kvantinį našumą[8]. Nepaisant gerų PhOLED charakteristikų, jie turi kelis kritinius trūkumus, tokius kaip brangi gamyba, toksiškumas, nepakankamas mėlynai šviečiančių prietaisų stabilumas, sunkiai išgaunamos grynos spalvos. Geras būdas padidinti PhOLED efektyvumą yra efektyvių matricinių medžiagų kūrimas. Itin efektyvios bipolinės matricinės medžiagos, skirtos OLED, gali būti sukurtos vienoje molekulėje, sujungiant skyles ir elektronus pernešančius fragmentus.

Termiškai aktyvuota uždelstąja fluorescencija (toliau – TADF) pasižyminčias medžiagas turintys OLED yra perspektyvūs gerinant šių prietaisų efektyvumą. TADF eksploatuojantys OLED pasižymi plačiu elektroliuminescencijos diapazonu, dideliu išoriniu kvantiniu efektyvumu, artimu fosforescencinių OLED efektyvumui. TADF mechanizmas gali būti realizuotas dėl grįžtamos interkombinacinės konversijos. TADF pasižymi 100% tripletinės būsenos energijos panaudojimu[30]. Efektyvių TADF spinduolių modeliavimo strategija daugiausia sutelkta ties sp^3 hibridizuotus azoto atomus turinčiais aromatiniais heterociklais (karbazolu, fentiazinu, fenoksazinu, akridanu ir kt.). Šiuos fragmentus turintys junginiai pasižymi geru terminiu ir elektrocheminiu stabilumu, geromis skylių pernašos savybėmis, stipriomis elektrondonorinėmis savybėmis ir didelės energijos tripletinėmis būsenomis.

Nepaisant sparčios organinės optoelektronikos plėtros ir gausybės organinių elektroaktyviųjų medžiagų, išlieka aktualios kai kurios problemos, tokios kaip brangi gamyba, trumpas eksploatavimo laikas (ypač ryškiai mėlynos emisijos OLED). Derinant skirtingus elektrondonorinius ir akceptorinius fragmentus, galima sukurti labai efektyvius organinius puslaidininkius. Parinkus tinkamus fragmentus, gali būti gaunamos efektyvios matricinės medžiagos, pasižyminčios didele tripletine energija, geromis skylių ir elektronų pernašos savybėmis, bei spinduoliai, pasižymintys efektyvia liuminescencija. Labai perspektyvūs yra spinduoliai, kuriems būdingas TADF reiškinys, agregacijos indukuota emisija (toliau – AIE), polimorfizmas ir mechanochromizmas arba šių savybių deriniai. Taigi, daugiafunkcinių organinių elektroaktyvių junginių panaudojimas gali leisti pagerinti elektroliuminescuojančių prietaisų, ypač mėlynų OLED, eksploatacines savybes.

Šio **darbo tikslas** – atlikti naujų donorinių-akceptorinių organinių darinių, skirtų organiniams šviesos diodams, savybių modeliavimą, sintezę ir ištirti jų savybes.

Tikslui pasiekti buvo iškelti šie **uždaviniai**:

• Susintetinti didelės tripletinės energijos karbazolo ir oksadiazolo darinius kaip matricines OLED medžiagas.

• Susintetinti akridano pakaitus turinčius perfluorbifenilo darinius kaip mėlynos ir žydros spalvos TADF spinduolius.

• Eksperimentiniais ir teoriniais metodais ištirti susintetintų junginių savybes.

• Įvertinti darinių, turinčių akridano ir perfluorbifenilo fragmentus, struktūros ir savybių tarpusavio priklausomybę.

• Ištirti naujų organinių boro kompleksų fotofizikines ir elektrochemines savybes.

• Įvertinti tikslinių junginių pritaikymo elektroliuminescenciniuose prietaisuose galimybes.

Darbo naujumas:

• Sumodeliuotos, susintetintos ir apibūdintos naujos karbazolo-oksadiazolo donorinės-akceptorinės matricinės medžiagos, kurios pritaikytos fosforescuojančiuose OLED.

• Sumodeliuoti, susintetinti ir apibūdinti nauji akridano ir perfluorbifenildariniai, pasižymintys termiškai aktyvuotąja uždelstąja fluorescencija bei agregacijos sustiprinta emisija, kurie pritaikyti OLED.

• Ištirta donorinių ir akceptorinių pakaitų, prijungtų prie benzotiazolo fragmento, įtaka naujų šviesą skleidžiančių organinių boro kompleksų fotofizikinėms savybėms.

4.2. PAGRINDINIAI REZULTATAI

4.2.1. W formos karbazolo-oksadiazolo darinių sintezė ir tyrimas

Sumodeliuotos ir susintetintos bipolinės matricinės medžiagos, turinčios karbazolo ir oksadiazolo fragmentus ir pasižyminčios didele tripletine energija. Gautų junginių **1–4** sintezė ir cheminės struktūros pateiktos 4.1 schemoje. Tiksliniai dariniai gauti temperatūros indukuotos reciklizacijos reakcijų *in situ* metu diacilbenzenditetrazolams virstant fenilendioksadiazolais. Susintetintų junginių **1–4** struktūros patvirtintos ^{1}H ir ^{13}C BMR spektroskopijos bei masių spektrometrijos metodais.

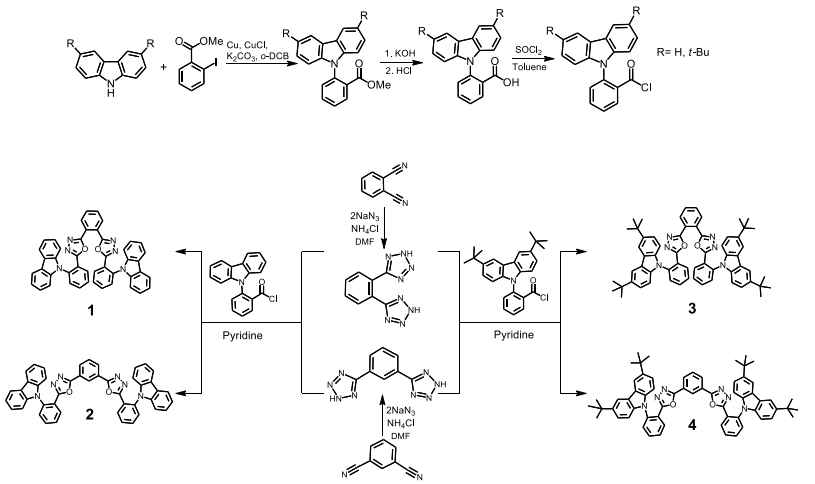

4.1 schema. Sintezės schema

Buvo atliktas karbazolo-oksadiazolo darinių savybių teorinis modeliavimas. Pritaikant tankio funkcionalo teoriją (DFT), optimizuotos molekulių **1–4** geometrinės konfigūracijos, jų molekulinių orbitalių lokalizacija pateikta 4.1 pav. Aukščiausios užimtos molekulinės orbitalės (toliau – HOMO) ir žemiausios laisvos molekulinės orbitalės (toliau – LUMO) yra atskirtos ir atitinkamai išdėstytos karbazolo ir fenildioksazolo fragmentuose.

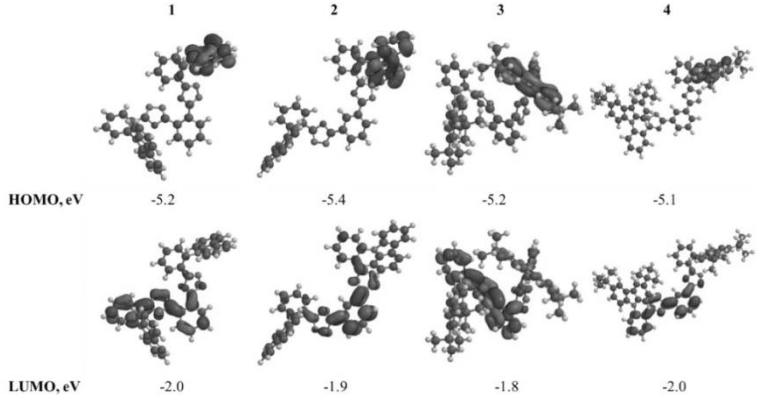

4.1 pav. Junginių **1–4** HOMO ir LUMO orbitalių pasiskirstymas bei energijos

Junginių **1–4** terminis stabilumas ir morfologinės savybės ištirtos termogravimetrinės analizės (toliau – TGA) ir diferencinės skanuojamosios kalorimetrijos (toliau – DSK) metodais. Jų 5 proc. masės nuostolio (T_{ID}), lydymosi (T_{lyd}) ir stiklėjimo (T_{st}) temperatūros apibendrintos 4.1 lentelėje. Visi susintetinti junginiai išskirti kaip kristalinės medžiagos. Pirmojo DSK kaitinimo metu pastebimos endoterminės lydymosi smailės temperatūros intervale 163–264 °C. *Tret*-butilpakeisto karbazolo dariniai (**3** ir **4**) pasižymi aukštesnėmis T_{ID} ir $T_{st,}$ palyginti su nepakeisto karbazolo dariniais (**1** ir **2**). Junginių **3** ir **4**, turinčių *tret*-butilgrupes, molekulinė masė yra didesnė, todėl padidėja T_{ID} ir T_{st}.

4.1 lentelė. Junginių **1–4** terminės, optinės ir fotofizikinės savybės

Jung.	T_{ID} [a], °C	T_{lyd} [b], °C	T_{st} [b], °C	λ_{abs} [c/d/e], nm	λ_{PL} [d/e/f], nm	Φ_{PL} [d]	Φ_{PL} [f]	E_S, eV	E_T, eV	ΔE_{S-T}
1	359	251	107	335/338 /337	429/427 /439	0,15	0,22	3,33	3,04	0,29
2	367	163	110	336/338 /337	427/445 /427	0,09	0,24	3,30	3,04	0,26
3	375	264	147	342/343 /344	442/440 /470	0,15	0,08	3,13	2,97	0,16
4	383	257	143	342/342 /342	443/438 /456	0,16	0,12	3,14	2,97	0,19

[a] Nustatyta TGA metodu. [b] Nustatyta DSC metodu. λ_{abs} – absorbcijos spektro maksimumas; λ_{PL} – fotoliuminescencijos spektro maksimumas; Φ – fotoliuminescencijos kvantinis našumas. [c] Dichlormetano tirpale. [d] Sluoksnyje. [e] Tolueno tirpale. [f] THF tirpale. E_S, E_T – atitinkamai singletinio ir tripletinio lygmenų energija.

Junginių praskiestų tirpalų ir sluoksnių absorbcijos (toliau – UV) ir fotoliuminescencijos (toliau – PL) spektrai pavaizduoti 4.2 pav. Junginių **1–4** tirpalų ir sluoksnių intramolekulinės krūvio pernašos absorbcijos smailės išsidėsčiusios ties 335–344 nm (4.1 lentelė). Visiems susintetintiems junginiams būdinga mėlyna emisija tolueno tirpaluose ir sluoksniuose bei bathochromiškai pasislinkusi emisija tetrahidrofurano (toliau – THF) tirpaluose. Junginių **1** ir **2**, turinčių nepakeistą karbazolo fragmentą, THF tirpalams būdingos šiek tiek didesnės PL kvantinių išeigų (toliau – *PLQY*) vertės nei junginių **3** ir **4**, turinčių *tret*-butilpakeistą karbazolo fragmentą (4.1 lentelė). Junginiams **1** ir **2** būdingas agregacijos sukeltas emisijos gesimas (toliau – ACQ, angl. *aggregation caused quenching*), kadangi jų sluoksnių *PLQY* vertės mažesnės, palyginti su atitinkamomis vertėmis praskiestuose THF tirpaluose. O junginiams **3** ir **4** būdinga agregacijos sustiprinta emisija.

Pirmųjų singletinio (toliau – E_S) ir tripletinio (toliau – E_T) lygmenų energijos, apskaičiuotos iš junginių THF tirpalų PL ir fosforescencijos (Ph) spektrų, užrašytų 77 K temperatūroje, E_S ir E_T vertės atitinkamai buvo 3,13–3,33 eV ir 2,97–3,04 eV (4.1 lentelė). Pastebėta, kad *tret*-butilpakaitas karbazolo-oksadiazolo dariniuose lėmė nedidelį tripletinės energijos sumažėjimą.

Buvo atlikti susintetintų junginių acetonitrilo tirpalų ciklinės voltamperometrijos (toliau – CV) tyrimai. Apskaičiuotos junginių **1–4** gimiringumo elektronui (toliau – EA_{CV}) vertės yra gana panašios (2,28–2,41 eV), o jonizacijos potencialo (toliau – IP_{CV}) vertės svyruoja nuo 5,46 eV iki 5,90 eV (4.2 lentelė). Įvertinti ir tiriamųjų junginių sluoksnių jonizacijos potencialai (toliau – IP_{PE}). Dėl

elektrondonorinių *tret*-butilgrupių junginiuose **3** ir **4** IP_{PE} vertės mažesnės, palyginti su nepakeistais analogais (junginiai **1** ir **2**). Taip pat apskaičiuotos junginių kietos būsenos gimiringumo elektronui (toliau – EA_{PE}) vertės (4.2 lentelė). Elektronų fotoemisijos ir CV metodu gautos *IP* ir *EA* vertės gerai koreliuoja tarpusavyje.

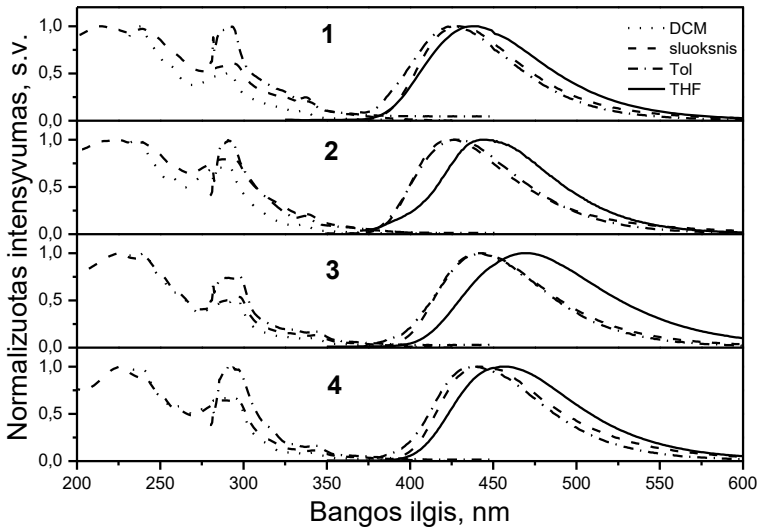

4.2 pav. Junginių praskiestų tirpalų ir sluoksnių UV bei PL (λ_{eks}= 330 nm) spektrai

4.2 lentelė. Junginių **1**–**4** elektrocheminės charakteristikos

Jung.	$E_{ox\ vs.\ Fc^+/Fc}^{pradžia}$	$E_{red\ vs.\ Fc^+/Fc}^{pradžia}$	$IP_{cv.}$, eV	EA_{CV}, eV	E_g, eV	IP_{PE}, eV	EA_{PE}, eV
1	0,92	–2,01	5,88	2,38	3,45	5,71	2,26
2	0,93	–2,10	5,90	2,28	3,43	5,71	2,28
3	0,76	–2,09	5,66	2,29	3,44	5,46	2,02
4	0,62	–1,99	5,46	2,41	3,42	5,52	2,10

$E_{ox\ vs.\ Fc^+/Fc}^{pradžia}$, $E_{red\ vs.\ Fc^+/Fc}^{pradžia}$ – atitinkamai oksidacijos ir redukcijos potencialų pradžia; *IP* – jonizacijos potencialas, $IP_{CV} = -1{,}4 * E_{ox}^{pradžia} - 4{,}60$; *EA* – gimiringumas elektronui, $EA_{CV} = -1{,}19 * E_{red}^{pradžia} - 4{,}78$; E_g – absorbcijos mažiausios energijos juostos krašto energija; IP_{PE} ir EA_{PE} – junginių sluoksnių atitinkamai jonizacijos potencialas ir gimiringumas elektronui; $EA_{PE} = IP_{PE} - E_g$.

Junginių **1**–**4** krūvininkų pernašos savybės tirtos lėkio trukmės (TOF) metodu (4.3a pav.). Visi susintetinti dariniai geba pernešti elektronus. Junginių **1** ir **4** elektronų judris mažesnis viena eile nei junginių **2** ir **3**. Be to, dariniai **2** ir **3** pasižymėjo bipoline krūvio pernaša. Krūvininkų judriai junginių sluoksniuose siekė 10^{-4} $cm^2V^{-1}s^{-1}$, esant vidutiniam elektros lauko stipriui. Junginiui **2** būdingas panašus skylių ir elektronų judris plačiame elektros lauko diapazone. Skirtingos intermolekulinės sąveikos tarp sluoksnyje esančių molekulių, vykstančios dėl įvairių pakaitų molekulėse, lėmė junginių **1**–**4** skylių ir elektronų judrio skirtumus.

Atsižvelgiant į aukštas tripletinės energijos vertes (iki 3,04 eV) bei bipolinį krūvininkų judrį, susintetinti junginiai panaudoti kaip matricinės medžiagos kartu su fosforescuojančiu spinduoliu bis(4',6'-difluorfenilpiridinato)–iridžio (III) pikolinatu

(toliau – FIrpic) formuojant mėlynus fosforescuojančius prietaisus. Pagaminti keli elektroliuminescenciniai (toliau – EL) prietaisai (A–E), jų pusiausvyrųjų energetinių lygmenų diagrama pateikta 4.3b pav. Visiems pagamintiems prietaisams būdingi panašūs EL spektrai, turintys FIrpic emisijos juostą, esant skirtingai įtampai. Geriausio pagaminto prietaiso, pasižyminčio gryna fosforescuojančio dažiklio emisija, išorinis kvantinis efektyvumas (toliau – EQE) buvo 8,8 proc. ir skaistis – 8700 cd/m^2, esant 10 V įtampai.

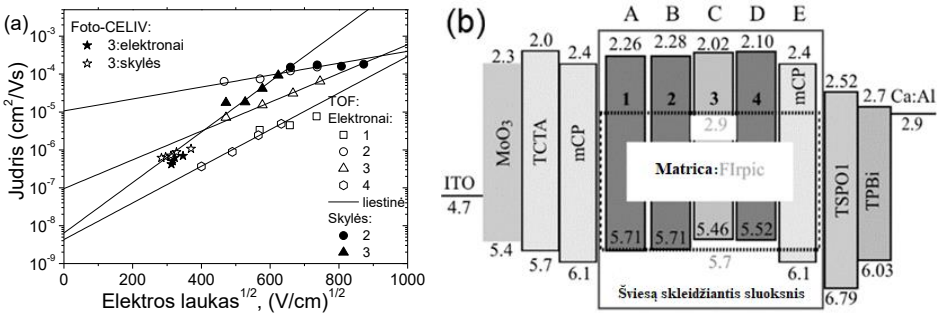

4.3 pav. Junginių **1**–**4** krūvininkų judrių priklausomybė nuo elektros lauko stiprio (a) bei prietaisų A–E energetinių lygmenų diagrama (b)

4.2.2. Polimorfinių *tret*-butilpakeisto akridano ir perfluorbifenilo darinių sintezė ir tyrimas

Susintetinti ir apibūdinti nauji mėlynai šviečiantys daugiafunkciniai liuminoforai, pasižymintys TADF, agregacijos sustiprinta emisija (toliau – AIEE) ir kintama emisijos spalva (mėlyna ↔ žydra). Pirmą kartą kaip akceptorius panaudotas perfluorbifenilas (PFBP). 9,9-dimetilakridanas (DMAC) pasirinktas dėl stiprių donorinių savybių. Taip pat, siekiant gauti junginius, turinčius geresnį terminį, morfologinį ir elektrocheminį stabilumą, panaudotas 2,7-di-*tret*-butil-9,9-dimetilakridanas. Keturių naujų D-A/D-A-D (angl. *donor-acceptor/donor-acceptor-donor*) tipo struktūros PFBP darinių sintezės schema pateikta 4.2 schemoje. Sintetinių junginių cheminės struktūros įrodytos ^{1}H, ^{13}C ir ^{19}F BMR spektroskopijos, kristalo rentgenostruktūrine analize ir ESI-MS masių spektrometrija.

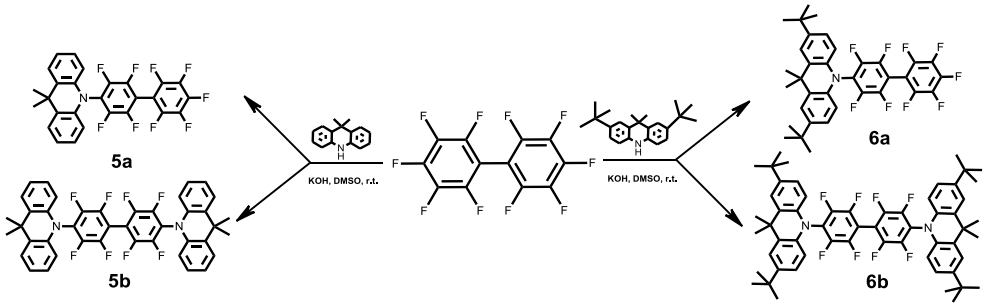

4.2 schema. Akridanpakeistų perfluorbifenilo darinių sintezė

Taip pat atlikti PFBP darinių savybių teoriniai skaičiavimai. HOMO ir LUMO orbitalių pasiskirstymas ir jų energetinės vertės pateiktos 4.4 pav.

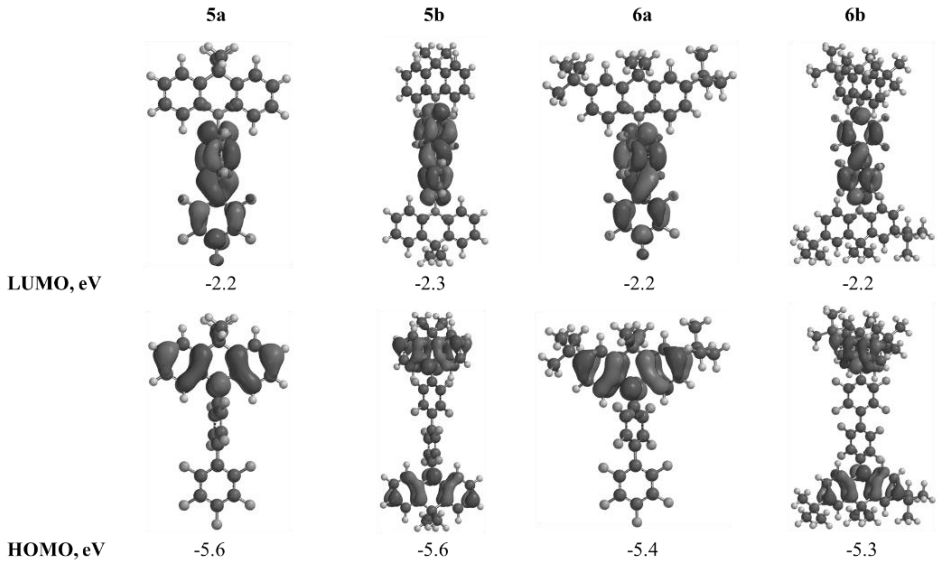

4.4 pav. Susintetintų PFBP junginių teoriniai skaičiavimai

PFBP darinių terminis stabilumas ir morfologinės savybės tirtos atitinkamai TGA ir DSK metodais. T_{ID}, T_{lyd}, T_{st} ir kristalizacijos temperatūros (toliau – T_{kr}) vertės apibendrintos 4.3 lentelėje. Tiksliniai junginiai, turintys D-A struktūrą (**5a** ir **6a**), pasižymi mažesnėmis T_{ID} ir T_{lyd}, palyginti su dariniais, turinčiais D-A-D struktūrą (**5b** ir **6**), dėl didelio fluoro, esančio PFBP fragmento C-10’ padėtyje, reaktyvumo monopakeistuose dariniuose. Visi susintetinti PFBP dariniai išskirti kaip kristalinės medžiagos. Be to, junginio **6a** pirmojo DSK kaitinimo metu pastebėtos dvi T_{lyd} vertės (212 ºC ir 221 ºC), galimai dėl dviejų skirtingų **6a** kristalinių struktūrų. Pažymėtina, kad po aušinimo ir antrojo kaitinimo ciklų T_{lyd} pastebimas tik esant 221 ºC.

4.3 lentelė. PFBP darinių terminės, elektrocheminės ir fotoelektrinės charakteristikos

Jung.	T_{ID}[a], °C	T_{lyd}[b], °C	T_{kr}, °C	T_{st}[d], °C	$E_{ox\ vs.\ Fc^+/Fc^{pradžios}}$	$E_{red\ vs.\ Fc^+/Fc^{pradžios}}$	IP_{CV}, eV	EA_{CV}, eV	IP_{PE}, eV
5a	205	189	121[c, d]	–	0,82	–2,17	5,75	2,19	6,43
5b	303	217	157[d]	98	0,83	–2,08	5,76	2,30	6,19
6a	232	212/221	109[d]	64	0,63	–2,21	5,48	2,15	5,92
6b	317	310	288[c]	–	0,62	–2,06	5,47	2,33	5,88

[a] Nustatyta TGA metodu. [b] DSK pirmas kaitinimo ciklas. [c] DSK šaldymo ciklas. [d] DSK antras kaitinimo ciklas. $E_{ox\ vs.\ Fc^+/Fc^{pradžios}}$, $E_{red\ vs.\ Fc^+/Fc^{pradžios}}$ – atitinkamai oksidacijos ir redukcijos potencialų pradžia; *IP* – jonizacijos potencialas; $IP_{CV} = -1{,}4 \times E^{pradžios}_{ox} - 4{,}60$; *EA* – gimiringumas elektronui; $EA_{CV} = -1{,}19 \times E^{pradžios}_{red} - 4{,}78$; IP_{PE} – sluoksnių jonizacijos potencialas.

Buvo atlikti junginių bevandenių DMF tirpalų CV matavimai ir apskaičiuotos IP_{CV} ir EA_{CV} vertės (4.3 lentelėje). Dariniai, turintys nepakeistus DMAC fragmentus (**5a** ir **5b**), pasižymi šiek tiek aukštesnėmis IP_{CV} reikšmėmis (5,75 eV ir 5,76 eV) nei *tret*-butilpakeistus DMAC fragmentus turintys junginiai **6a** ir **6b** (5,48 eV ir 5,47 eV),

tai koreliuoja su teoriniais skaičiavimais. D-A (**5a** ir **6a**) ir D-A-D (**5b** ir **6b**) tipo medžiagos pasižymi panašiomis EA_{CV} reikšmėmis (atitinkamai 2,19 eV ir 2,13 eV; 2,30 eV ir 2,33 eV, 2.4 lentelė). Kietų PFBP sluoksnių IP_{PE} vertės didesnės už CV metodu nustatytas *IP* vertes (4.3 lentelė), tikriausiai dėl skirtingos PFBP darinių praskiestų tirpalų ir sluoksnių molekulinės sąveikos ir išdėstymo. Junginių **6a** ir **6b** IP_{PE} ir IP_{CV} vertės yra šiek tiek mažesnės nei **5a** ir **5b** dėl *tret*-butilgrupių elektrondonorinio efekto.

Tikslinių PFBP darinių UV-Vis ir PL spektrai skirtingose terpėse pavaizduoti 4.5a pav. Absorbcijos ir emisijos juostų maksimumai pateikti 4.4 lentelėje. PFBP darinių tolueno ir THF tirpalų ICT (angl. *intramolecular charge transfer*) absorbcijos juostos išsidėsčiusios tarp 348 nm ir 371 nm. *Tret*-butilpakeistus DMAC fragmentus turinčių darinių (**6a** ir **6b**) sluoksnių absorbcijos juostos pasižymi nedideliais bathochrominiais poslinkiais, palyginti su atitinkamomis jų praskiestų tirpalų juostomis, dėl tarpmolekulinių sąveikų esant kietai būsenai.

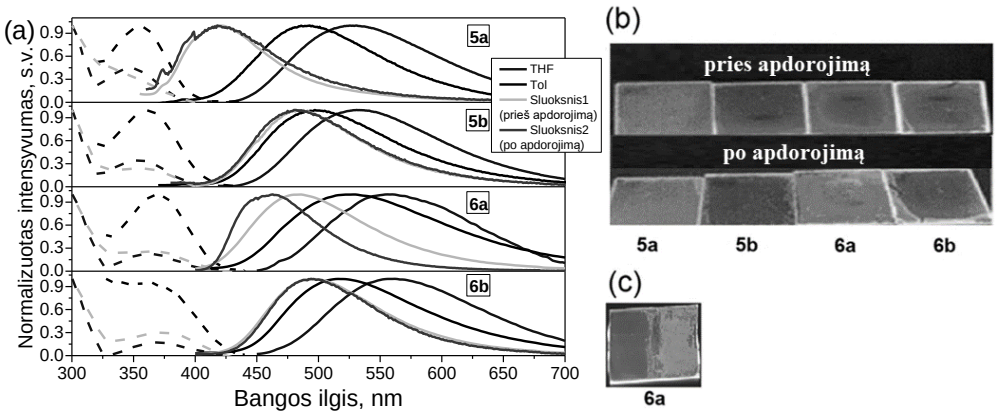

4.5 pav. PFBP darinių tolueno ir THF tirpalų bei sluoksnių prieš ir po apdorojimo tolueno garais UV ir PL spektrai (a). Sluoksnių emisijos spalva prieš ir po apdorojimo tolueno garais (b); junginio **6a** sluoksnis neapdorotas (kairė pusė) ir mechaniškai bei temperatūra (< 80 °C) apdorotas (dešinėje pusėje), veikiant UV spinduliuote (c)

4.4 lentelė. PFBP darinių fotofizikinės savybės

Jung.	$\lambda_{abs}^{a/b/c}$, nm	$\lambda_{PL}^{a/b/c}$, nm	Φ_{PL}^{a}	Φ_{PL}^{c}
5a	348/356/356	531/493/418	0,04[a]	0,27
5b	355/362/362	531/497/482	0,1[a]	0,34
6a	364/371/371	556/528/486[d],463[e]	0,03[b]	0,43[d]/ 0,61[e]
6b	370/364/376	562/516/494	0,08[b]	0,46

[a] THF tirpale. [b] Tolueno tirpale. [c] Sluoksnyje. [d] Vakuuminiu nusodinimu gauti (amorfiniai) sluoksniai prieš apdorojant juos tolueno garais. [e] Vakuuminiu nusodinimu gauti (kristaliniai) sluoksniai po apdorojimo tolueno garais. λ_{abs} – absorbcijos spektro maksimumas; λ_{PL} – PL spektro maksimumas; Φ – PL kvantinis našumas.

PFBP darinių emisijai būdingas stiprus solvatochrominis efektas, kuris nulėmė bathochrominius PL spektrų poslinkius didelio poliškumo tirpikliuose (4.5a pav.). *Tret*-butilpakeistus DMAC fragmentus turinčių junginių (**6a** ir **6b**) sluoksniai

pasižymi žydra emisija, o junginių, turinčių nepakeistus DMAC fragmentus (**5a** ir **5b**), sluoksniai atitinkamai emituoja mėlynoje ir žydroje spektro srityse (4.5a pav., 4.4 lentelė). Visų PFBP darinių sluoksnių emisijoje pastebėtas hipsochrominis poslinkis, palyginti su jų THF ir tolueno tirpalų emisija (4.5a pav.). Be to, **6a** sluoksnį apdorojus tolueno garais, pastebėtas didesnis hipsochrominis emisijos pokytis (4.5b pav.). Taip pat **6a** sluoksniui būdingos mechanochrominės (MCL) savybės: emisijos spalva (žydra ↔ mėlyna) kinta veikiant išoriniams veiksniams (mechaninei jėgai arba temperatūrai) (4.5c pav.). Visiems gautiems junginiams būdingos didesnės kietosios būsenos *PLQY* vertės, palyginti su jų tirpalais, dėl AIEE efekto.

Atlikus kristalų rentgeno spindulių difrakcijos analizę, buvo aptiktos dvi junginio **6a** kristalinės atmainos, A ir B (4.6 pav.). Pagrindinis skirtumas tarp **6a**_A ir **6a**_B kristalinių struktūrų yra metilgrupių struktūrinė deformacija 9-toje *tret*-butilpakeisto DMAC padėtyje **6a**_B kristaluose. **6a**_B kristale atstumas tarp atitinkamo vandenilio atomo ir artimiausio fluoro atomo yra daug mažesnis (2,814 Å), palyginti su atitinkamu C-H···F atstumu kristale **6a**_A (4,104 Å). Palyginus šiuos atstumus su fluoro ir vandenilio atomų Van der Waals spindulių suma (2,67 Å), išmatuotas C-H···F atstumas kristale **6a**_B yra labai artimas minimaliai vertei, reikalingai vandeniliam ryšiui sudaryti (4.6 pav.). Atsižvelgdami į fizikinių savybių skirtumus, galime daryti išvadą, kad šis ryšys yra susidaręs ir turi įtakos fotofizikinėms bei terminėms savybėms, o nedidelis skirtumas tarp C-H···F atstumo kristale **6a**_B ir Van der Waals spindulių sumos yra slopinamas molekulinių vibracijų sudarant silpną vandenilinį ryšį kristale **6a**_B.

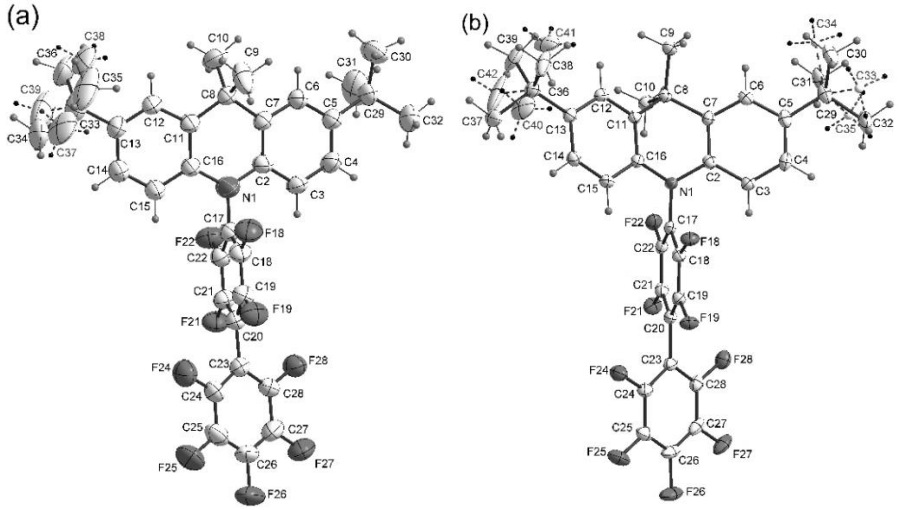

4.6 pav. Asimetrinių kristalų **6a**_A (a) ir **6a**_B (b) atomų numeravimo schema

Pagaminti keli OLED panaudojant naujus TADF spinduolius (**5b**, **6a** ir **6b**) (4.7 pav.). Be to, junginys **6b** naudotas nelegiruoto prietaiso gamyboje dėl jo didžiausios *PLQY* vertės kietajame būvyje. Pagamintų prietaisų EL spektrų maksimumai išsidėsto žydros ir žalsvai mėlynos spalvos regionuose (2.5 lentelė). Legiruotų prietaisų (A, B ir D) įsijungimo įtampa yra daug mažesnė (atitinkamai 3,8 V, 3,9 V ir 3,0 V) nei nelegiruoto prietaiso C (7,0 V). Aukšta prietaiso C įjungimo

įtampa pasiekta dėl nelegiruoto **6b** sluoksnio stipriai dispersinės krūvininkų pernašos. Geriausias pagamintas OLED pasiekė maksimalias *EQE* – 16,3 proc., srovės efektyvumo (*CE* (η_c) – angl. *current efficiency*) – 30,8 cd/A ir galios efektyvumo (*PE* (η_p) – angl. *power efficiency*) – 22,7 lm/W vertes (4.5 lentelė).

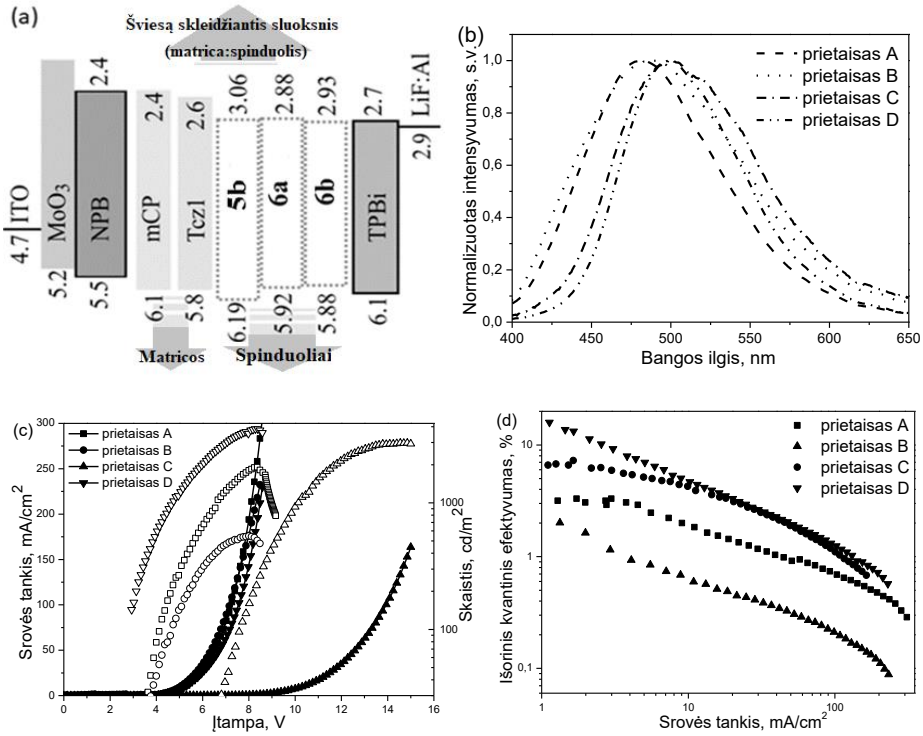

4.7 pav. Prietaisų A-D pusiausvyros energijos lygio diagramos (a), EL spektrai (b), srovės tankio ir skaisčio priklausomybė nuo įtampos (c) bei išorinio kvantinio efektyvumo ir srovės tankio tarpusavio priklausomybė (d)

4.5 lentelė. OLED-ų charakteristikos

Prietaisa	$V_{ijung.}$, V	Maks. skaistis, Cd/m^2	η_c^{max}, Cd/A	η_p^{max}, lm/W	EQE^{max}, pr oc.	λ_{max}^{EL},nm	*CIE*, (x, y)
A	3,8	1850	6,5	4,4	3,3	480*	(0,177, 0,266)*
B	3,9	550	3,7	2,5	3,9	487*	(0,199, 0,289)*
C	7,0	3000	16,3	5,8	6,6	499**	(0,222, 0,388)**
D	3,0	3900	30,8	22,7	16,3	499*	(0,202, 0,419)*

* esant 6V. ** esant 12 V. Prietaisų struktūros: A – ITO/MoO_3/NPB/**5b**:mCP/TPBi/Ca/Al; B – ITO/MoO_3/NPB/**6a**:TCz1/TPBi/Ca/Al; C – ITO/MoO_3/NPB/**6b**/TPBi/Ca/Al; D – ITO/MoO_3/NPB/**6b**:TCz1/TPBi/Ca/Al.

4.2.3. Organinių boro kompleksų (benz[4,5]tiazol[3,2-c][1,3,5,2]-oksadiazaborininų) fotofizikinių savybių tyrimas

Dvi junginių grupės, turinčios benz[4,5]tiazol[3,2-c][1,3,5,2]-oksadiazaborininų fragmentus (4.8 pav.), sumodeliuotos ir susintetintos dr. M. A. Potopnyk. Ištirtos jų fotofizikinės ir elektrocheminės savybės.

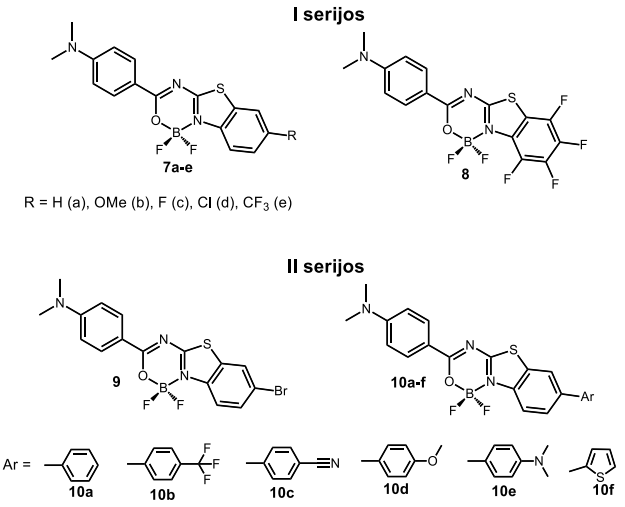

4.8 pav. Tirtų organinių boro kompleksų cheminės struktūros

I serijos **7a–e** ir **8** junginių bei II serijos **9** ir **10a–f** junginių praskiestų tirpalų ir sluoksnių absorbcijos ir PL spektrai pateikti atitinkamai 4.9a ir b paveiksluose. Absorbcijos ir emisijos spektrų maksimumai apibendrinti 4.6 lentelėje. Tirtiems I serijos darinių (**7a-e** ir **8**) tirpalams būdinga viena absorbcijos smailė, esanti 411–434 nm srityje, atitinkanti $S_0 \rightarrow S_1$ perėjimą. Tiriamiems II serijos junginių (**9** ir **10a-f**) tirpalams būdinga viena absorbcijos smailė violetinės ir mėlynos spalvos srityje, ties 427–439 nm.

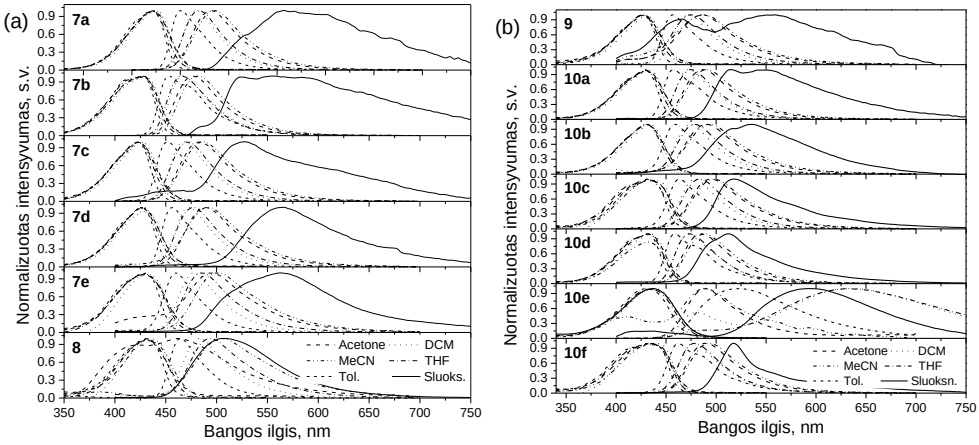

4.9 pav. Junginių **7a-e**, **8** (a) ir **9**, **10a-f** (b) UV/Vis ir PL spektrai

Visi I serijos organiniai boro kompleksai pasižymėjo solvatochromizmo efektu: didėjant tirpiklio poliškumui nuo tolueno iki acetonitrilo, pastebimas batochrominis emisijos spektro poslinkis (4.9a pav.). Pastebėta benztiazolo elektroninės struktūros įtaka fotofizikinėms savybėms (4.6 lentelė). Junginiams **7a–e** tolueno tirpaluose būdinga aukšta *PLQY* vertė (0,84–0,93), o junginiui **8** būdingas mažesnis PL efektyvumas (0,65). Visų tirtų organinių boro kompleksų *PLQY* vertė mažėjo, didėjant tirpiklio poliškumui (4.6 lentelė lentelė). Junginių **7a-e** ir **8** sluoksnių PL spektrai yra batochromiškai pasislinkę, payginti su tirpalų spektrais (4.9a pav.). Junginių **7a-e** sluoksnių *PLQY* vertės yra labai žemos (0,02–0,06), o junginio **8** sluoksnio santykinai aukštą Φ_{PL} (0,34) nulėmė specifinė tarpmolekulinė sąveika ir molekulių susipakavimas. Taip pat nustatytos junginių tolueno tirpalų ir sluoksnių sužadintos būsenos gyvavimo trukmės (toliau – τ) bei rezultatai pateikti 4.7 lentelėje.

4.6 lentelė. Junginių **7a–e, 8, 9, 10a–f** fotofizikinės charakteristikos

Jung.	λ_{abs}[a/b/c/d/e], nm	λ_{PL}[a/b/c/d/e/f], nm	Φ_{PL}[a/b/c/d/e/f]
7a	425/425/421/424/421	482/467/468/469/450/557	0,31/0,77/0,17/0,78/0,84/0,03
7b	431/430/426/430/411,427	477/467/481/466/454/555	0,56/0,83/0,38/0,80/0,88/0,05
7c	426/425/422/425/423	483/468/487/472/452/528	0,23/0,74/0,13/0,72/0,85/0,02
7d	430/430/426/430/427	488/473/491/477/456/566	0,21/0,78/0,12/0,74/0,91/0,02
7e	431/431/427/430/428	495/478/500/486/460/563	0,13/1/0,05/0,61/0,93/0,03
8	432/433/431/434/431	463/483/503/492/464/506	0,06/0,66/0,02/0,47/0,65/0,34
9	427/431/430/426/427	482/467/486/469/450/464,559	0,27/0,61/0,13/0,55/0,74/0,03
10a	430/432/430/430/430	487/473/491/475/457/515	0,56/0,74/0,33/0,82/0,92/0,17
10b	430/434/430/430/431	490/475/493/479/459/536	0,42/0,74/0,29/0,75/0,80/0,07
10c	432/436/432/431/434	490/475/493/479/459/518	0,55/0,98/0,32/0,96/0,99/0,31
10d	432/437/431/431/431	485/473/488/474/459/536	0,65/0,79/0,43/0,82/0,95/0,06
10e	436/438/435/433/430	490/480,631/487/487,630/523/667	0,01/0,04/0,02/0,03/0,78/0,12
10f	435/439/435/436/436	489/477/493/478/462/518	0,65/0,91/0,44/0,87/0,84/0,13

[a] Acetono tirpalas. [b] Dichlormetano (DCM) tirpalas. [c] Acetonitrilo tirpalas. [d] THF tirpalas. [e] Tolueno tirpalas. [f] Sluoksnis. λ_{abs} – absorbcijos spektro maksimumas; λ_{PL} – PL spektro maksimumas; Φ – PL kvantinis našumas.

Visiems II serijos darinių, išskyrus **10e**, praskiestiems tirpalams būdinga viena emisijos juosta. Junginio **10e** didelės ir mažos energijos emisijos juostų intensyvumas labai priklauso nuo terpės poliškumo. Organinių boro kompleksų **9** ir **10a–f** sluoksnių fluorescencijos spektrai yra batochromiškai pasislinkę, palyginti su atitinkamais jų praskiestais tirpalais (4.9b pav.). Ištirtas kompleksų **9** ir **10a–f** praskiestų tirpalų ir sluoksnių PL efektyvumas ir atitinkamos *QY* vertės pateiktos 4.6 lentelėje. Visų tirtų darinių tolueno tirpaluose buvo didelė *PLQY* vertė (0,74–0,99), o, padidinus tirpiklio poliškumą, PL efektyvumas sumažėjo (4.6 lentelė). Junginio **10e** visuose tirpaluose, išskyrus tolueno, pastebėtas PL gesimas (*PLQY* 0,01–0,04), sukeltas didelio ICT efekto. Priešingai nei tolueno tirpaluose, pastebima silpna tiriamų kompleksų **9**, **10a**, **b**, **d–f** sluoksnių *PLQY* (0,03–0,17), tikriausiai susijusi su ACQ efektu dėl tankaus

molekulinio susipakavimo. Be to, junginio **10c** sluoksnis pasižymi gana aukšta Φ verte (0,31). Šio efekto priežastis gali būti paaiškinta ACQ sumažėjimu, kurį sukelia šio junginio molekulinio susipakavimo specifiškumas. Nustatyti kompleksų **9** ir **10a–f** tolueno tirpalų ir sluoksnių τ, rezultatai pateikti 4.7 lentelėje.

4.7 lentelė. Junginių **7a–e, 8, 9, 10a–f** fotofizikinės ir elektrocheminės charakteristikos

Jung.	τ, ns[a/b]	χ [a/b]	$E_{ox\ vs.\ Fc^+/Fc\ pradžios}$	$E_{red\ vs.\ Fc^+/Fc\ pradžios}$	IP_{CV}, eV	EA_{CV}, eV
7a	1,74/0,81;4,10	1,017/1,001	0,72	-2,00	5,12	2,40
7b	1,59/0,88;4,36	1,190/1,015	0,72	-1,99	5,12	2,41
7c	1,68/0,66;3,38	1,177/1,008	0,73	-1,95	5,13	2,45
7d	1,71/1,04;5,90	1,049/1,015	0,73	-1,92	5,13	2,48
7e	1,78/0,99;2,64	1,003/1,148	0,76	-1,83	5,16	2,57
8	2,00/1,77;7,56	1,017/1,002	0,78	-1,65	5,18	2,75
9	1,61/0,65;3,28	1,009/1,018	0,71	-1,90	5,11	2,50
10a	1,43/1,11;4,51	1,099/1,053	0,71	-1,94	5,11	2,46
10b	1,41/1,04;3,87	1,142/1,029	0,70	-1,91	5,10	2,49
10c	1,45/1,12;4,01	1,008/1,003	0,73	-1,88	5,13	2,52
10d	1,39/0,34;2,26	1,018/1,014	0,70	-2,03	5,10	2,37
10e	1,96/0,61;3,86	1,114/1,164	0,24	-1,95	4,64	2,45
10f	1,31/0,69;1,71	1,024/1,272	0,44/0,60	-1,52	4,84/5,00	2,88

τ – sužadintos būsenos gyvavimo trukmė. χ – apskaičiuota paklaida. [a] Tolueno tirpalas. [b] Sluoksnis. $E_{ox\ vs.\ Fc^+/Fc^{pradžios}}$, $E_{red\ vs.\ Fc^+/Fc^{pradžios}}$ – atitinkamai oksidacijos ir redukcijos potencialų pradžia; *IP* – jonizacijos potencialas; $IP_{CV} = E^{onset}_{ox} + 4{,}40$. *EA* – gimininguma elektronui; $EA_{CV} = E^{onset}_{red} + 4{,}40$.

Ištirtos tiriamųjų kompleksų dichlormetano tirpalų elektrocheminės savybės ir gautos I ir II serijų CV kreivės pateiktos atitinkamai 4.10a ir b pav. IP_{CV} ir EA_{CV} vertės apibendrintos 4.7 lentelėje. Junginių **7a–e** ir **8** IP_{CV} ir EA_{CV} vertės atitinkamai buvo 5,12–5,18 eV ir 2,40–2,75 eV. Junginių **9** ir **10a–d** IP_{CV} vertės yra panašios (5,10–5,13 eV), o dariniai **10e** ir **10f** pasižymi daug mažesnėmis IP_{CV} vertėmis (atitinkamai 4,64 eV ir 4,84/5,00 eV). Apskaičiuotos junginių **9** ir **10a–e** EA_{CV} vertės svyruoja nuo 2,37 eV iki 2,52 eV, o junginio **10f** nustatyta daug didesnė EA_{CV} vertė (2,88 eV).

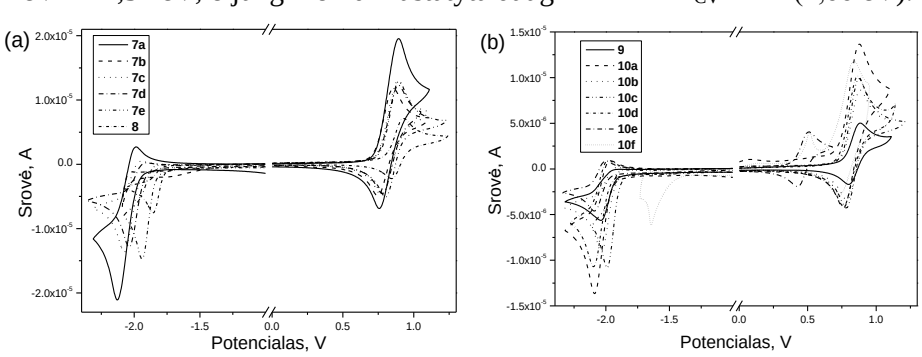

4.10 pav. Junginių **7a-e**, **8** (a) ir **9**, **10a-f** (b) elektrocheminės savybės

4.3. IŠVADOS

1. Susintetinti mėlynai fluorescuojantys W formos karbazolo ir oksadiazolo dariniai, turintys skirtingai pakeistus benzeno žiedus, kurie panaudoti kaip OLED matricos. Siekiant pagerinti junginių terminį ir morfologinį stabilumą, *tret*-butilgrupės prijungtos prie karbazolo fragmento. Nustatyta, kad:

1.1. Dariniams, turintiems *tret*-butilpakeistus karbazolo fragmentus, būdingos aukštesnės 5% masės nuostolių ir stiklėjimo temperatūros vertės negu atitinkamų junginių, turinčių nepakeistus karbazolo fragmentus (atitinkamai 383 °C ir 147 °C).

1.2. Junginiams būdinga didelė tripletinė energija (2,97–3,04 eV). Elektrondonoriniai *tret*-butilpakaitai neturi reikšmingos įtakos tripletinei energijai.

1.3. Junginių sluoksniai geba pernešti elektronus. Du junginiai turi bipolinę krūvininkų pernašą, su subalansuotais skylių ir elektronų judriais, kurie siekia 1×10^{-4} cm^2/V, esant dideliam elektros lauko stipriui.

1.4. Karbazolo ir oksadiazolo dariniai yra tinkami naudoti kaip matricos mėlynos šviesos fosforescenciniuose OLED. Geriausias pagamintas prietaisas pasižymėjo gryna fosforescencinio spinduolio emisija ir pasiekė 8,8 proc. išorinio kvantinio efektyvumo ir 8700 cd/m^2 skaisčio vertes, esant 10 V įtampai.

2. Susintetinti keturi nauji donoro-akceptoriaus ir donoro-akceptoriaus-donoro struktūros dariniai, turintys perfluorbifenilo ir akridano fragmentus, kurie panaudoti formuojant OLED kaip mėlynos ir žydros spalvos TADF spinduoliai. Nustatyta, kad:

2.1. Junginiai pasižymi vidutiniu terminiu stabilumu: jų 5 proc. masės nuostolių temperatūra viršijo 317 °C; du junginiai geba formuoti molekulinius stiklus, jų stiklėjimo temperatūros yra 64 ir 98 °C. Donoro-akceptoriaus-donoro struktūros junginiai pasižymi aukštesnėmis 5 proc. masės nuostolių, lydymosi ir kristalizacijos temperatūromis, palyginti su donoro-akceptoriaus struktūros dariniais.

2.2. Kietos būsenos junginiai pasižymi mėlyna ir žydra emisija, emisijos maksimumams esant intervale nuo 418 iki 494 nm. Junginiai, turintys išplėstą π-konjugaciją (donoro-akceptoriaus-donoro struktūra) ir papildomus elektrondonorinius *tret*-butilpakaitus, pasižymi emisijos batochrominiais poslinkiais ir didesniu fotoliuminescencijos efektyvumu.

2.3 Vieno iš susintetintų junginių molekulinio mišinio su matrica, turinčia didelę tripletinę energiją, fotoliuminescencijos kvantinis našumas siekė 73 proc. Perfluorbifenilo dariniai pasižymi termiškai aktyvuota uždelstąja fluorescencija ir agregacijos sustiprinta emisija.

2.4. Vienas iš gautų junginių sudarė dvi kristalines atmainas, kurios pasižymėjo skirtinga emisijos spalva bei spalvos kitimu, veikiant išoriniams veiksniams, jų sluoksnių fotoliuminescencijos kvantinis našumas buvo 43 ir 61 proc.

2.5. Perfluorbifenilo dariniai yra tinkami naudoti kaip mėlynos/žydros spalvos TADF spinduoliai OLED prietaisuose. Efektyviausias pagamintas elektroliuminescencinis prietaisas pasižymėjo žema 3 V įjungimo įtampa bei

maksimaliais srovės, galios ir išoriniu kvantiniu efektyvumais, atitinkamai – 22,7 cd/A, 30,8 lm/W ir 16,3 proc.

3. Ištirtos dviejų serijų organinių boro kompleksų fotofizikinės ir elektrocheminės savybės. Nustatyta, kad:

3.1. Tirti organiniai boro kompleksai pasižymi solvatochromizmu. Junginių tirpalų nepoliniuose tirpikliuose fotoliuminescencijos kvantinis našumas yra 65–100 proc. Vieno iš organinių boro kompleksų sluoksnis pasižymi vidutiniu fotoliuminescencijos kvantiniu našumu (34 proc.). Junginių jonizacijos potencialų ir gimiringumo elektronui vertės, nustatytos ciklinės voltametrijos metodu, atitinkamai buvo nuo 5,12 eV iki 5,18 eV ir nuo 2,40 eV iki 2,75 eV.

3.2. Ištirtų medžiagų tirpalams skirtinguose tirpikliuose būdinga viena emisijos juosta, o organinių boro kompleksų tirpalų nepoliniuose tirpikliuose fotoliuminescencijos kvantinis našumas yra 78–99 proc. Vieno iš tiriamų darinių tirpalams poliniuose tirpikliuose būdingos dvi emisijos juostos. Junginių jonizacijos potencialų ir gimiringumo elektronui vertės, nustatytos ciklinės voltamperometrijos metodu, atitinkamai buvo nuo 4,64 eV iki 5,13 eV ir nuo 2,37 eV iki 2,88 eV.

5. REFERENCES

1. BERGGREN, M., et al. Organic materials for printed electronics. *Nature Materials* [interactive]. 2007, vol. 6(1), 3–5. Access via the Internet: <https://dx.doi.org/10.1038/nmat1817>.

2. Embracing the organics world. *Nature Materials* [interactive]. 2013, vol. 12(7), 591–591. Access via the Internet: < https://dx.doi.org/10.1038/nmat3707>.

3. TAKIMIYA, K., et al. π-Building blocks for organic electronics: revaluation of "inductive" and "resonance" effects of π-electron deficient units. *Chemistry of Materials* [interactive]. 2013, vol. 26(1), 587–593. Access via the Internet: <https://dx.doi.org/10.1021/cm4021063>.

4. JOU, J.-H., et al. Approaches for fabricating high efficiency organic light emitting diodes. *Journal of Materials Chemistry C* [interactive]. 2015, vol. 3(13), 2974–3002. Access via the Internet: <https://doi.org/10.1039/C4TC02495H>.

5. GEFFROY, B., et al. Organic light-emitting diode (OLED) technology: materials, devices and display technologies. *Polymer International* [interactive]. 2006, vol. 55(6), 572–582. Access via the Internet: <https://doi.org/10.1002/pi.1974>.

6. LUNDIN, N. J., et al. Synthesis and characterization of a multicomponent rhenium(I) complex for application as an OLED dopant. *Angewandte Chemie International Edition* [interactive]. 2006, vol. 45(16), 2582–2584 Access via the Internet: <https://doi.org/10.1002/anie.200504532>.

7. LIU, W., et al. Novel carbazol-pyridine-carbonitrile derivative as excellent blue thermally activated delayed fluorescence emitter for highly efficient organic light-emitting devices. *ACS Applied Materials & Interfaces* [interactive]. 2015, vol. 7(34), 18930–18936. Access via the Internet: <https://dx.doi.org/10.1021/acsami.5b05648>.

8. SHIH, P.-I., et al. Novel host material for highly efficient blue phosphorescent OLEDs. *Journal of Materials Chemistry* [interactive]. 2007, vol. 17(17), 1692–1698. Access via the Internet: <https://doi.org/10.1039/b616043c>.

9. LYU, Y.-Y., et al. Highly efficient red phosphorescent OLEDs based on non-conjugated silicon-cored spirobifluorene derivative doped with Ir-complexes. *Advanced Functional Material*s [interactive]. 2009, vol. 19(3), 420–427. Access via the Internet: <https://doi.org/10.1002/adfm.200801319>.

10. HSU, F.-M., et al. A bipolar host material containing triphenylamine and diphenylphosphoryl-substituted fluorene units for highly efficient blue electrophosphorescence. *Advanced Functional Materials* [interactive]. 2009, vol. 19(17), 2834–2843. Access via the Internet: <https://doi.org/10.1002/adfm.200900703>.

11. TAO, Y., et al. Morphologically and electrochemically stable bipolar host for efficient green electrophosphorescence. *Physical Chemistry Chemical Physics* [interactive]. 2010, vol. 12(10), 2438–2442. Access via the Internet: <https://doi.org/10.1039/b922110g>.

12. TAO, Y., et al. Organic host materials for phosphorescent organic light-emitting diodes. *Chemical Society Reviews* [interactive]. 2011, vol. 40(5), 2943–2970. Access via the Internet: <https://doi.org/10.1039/c0cs00160k>.

13. NISHIMOTO, T., et al. A six-carbazole-decorated cyclophosphazene as a host with high triplet energy to realize efficient delayed-fluorescence OLEDs. *Materials Horizons* [interactive]. 2014, vol. 1(2), 264–269. Access via the Internet: <https://doi.org/10.1039/c3mh00079f>.

14. BONESI, S. M., and ERRA-BALSELLS, R. Electronic spectroscopy of N- and C-substituted chlorocarbazoles in homogeneous media and in solid matrix. *Journal of Luminescence* [interactive]. 2002, vol. 97(2), 83–101. Access via the Internet: <https://doi.org/10.1016/s0022-2313(01)00240-x>.

15. WEX, B., and KAAFARANI, B. R. Perspective on carbazole-based organic compounds as emitters and hosts in TADF applications. *Journal of Materials Chemistry C* [interactive]. 2017, vol. 5(34), 8622–8653. Access via the Internet: <https://doi.org/10.1039/c7tc02156a>.

16. WAGNER, D. et al. Triazine based bipolar host materials for blue phosphorescent OLEDs. *Chemistry of Materials* [interactive]. 2013, vol. 25(18), 3758–3765. Access via the Internet: < https://doi.org/10.1021/cm4023216>.

17. KIM, M. et al. Molecular design of triazine and carbazole based host materials for blue phosphorescent organic emitting diodes. *Physical Chemistry Chemical Physics* [interactive]. 2015, vol. 17(20), 13553–13558. Access via the Internet: <https://doi.org/10.1039/C5CP01676B>.

18. LIU, X.-K. et al. Novel bipolar host materials based on 1,3,5-triazine derivatives for highly efficient phosphorescent OLEDs with extremely low efficiency roll-off. *Physical Chemistry Chemical Physics.* [interactive]. 2012, vol. 14(41), 14255. Access via the Internet: <https://doi.org/10.1039/C2CP41542A>.

19. TAO, Y. et al. Dynamically adaptive characteristics of resonance variation for selectively enhancing electrical performance of organic semiconductors. *Angewandte Chemie International Edition* [interactive]. 2013. vol. 52(40), 10491–10495. Access via the Internet: < https://doi.org/10.1002/anie.201304540>.

20. SU, S.-J. et al. Pyridine-containing bipolar host materials for highly efficient blue phosphorescent OLEDs. *Chemistry of Materials* [interactive]. 2008. vol. 20(5), 1691–1693. Access via the Internet: <http://dx.doi.org/10.1021/cm703682q>.

21. HUANG, H., et al. Simple phenanthroimidazole/carbazole hybrid bipolar host materials for highly efficient green and yellow phosphorescent organic light-emitting diodes. *The Journal of Physical Chemistry C* [interactive]. 2012, vol. 116(36), 19458–19466. Access via the Internet: <https://doi.org/10.1021/jp305764b>.

22. TING, H.-C., et al. Indolo[3,2-b]carbazole/benzimidazole hybrid bipolar host materials for highly efficient red, yellow, and green phosphorescent organic light emitting diodes. *Journal of Materials Chemistry* [interactive]. 2012, vol. 22(17), 8399–8407. Access via the Internet: <https://doi.org/10.1039/c2jm30207a>.

23. CHENG, S.-H., et al. Highly twisted biphenyl-linked carbazole–benzimidazole hybrid bipolar host materials for efficient PhOLEDs. *Journal of Materials Chemistry C* [interactive]. 2014, vol. 2(40), 8554–8563. Access via the Internet: <https://doi.org/10.1039/c4tc01463d>.

24. TAO, Y., et al. Molecular design of host materials based on triphenylamine/oxadiazole hybrids for excellent deep-red phosphorescent organic light-emitting diodes. *Journal of Materials Chemistry* [interactive]. 2010, vol. 20(9), 1759–1765. Access via the Internet: <https://dx.doi.org/10.1039/b920227g>.

25. TAO, Y., et al. A simple carbazole/oxadiazole hybrid molecule: an excellent bipolar host for green and red phosphorescent OLEDs. *Angewandte Chemie International Edition* [interactive]. 2008, vol. 47(42), 8104–8107. Access via the Internet: <https://dx.doi.org/10.1002/anie.200803396>.

26. KAUTNY, P., et al. Oxadiazole based bipolar host materials employing planarized triarylamine donors for RGB PHOLEDs with low efficiency roll-off. *Journal of Materials Chemistry C* [interactive]. 2014, vol. 2(11), 2069–2081. Access via the Internet: <https://dx.doi.org/10.1039/c3tc32338b>.

27. AHN, J. H., et al. Organic light-emitting diodes based on a blend of poly[2-(2-ethylhexyloxy)-5-methoxy-1,4-phenylenevinylene] and an electron transporting material. *Applied Physics Letters* [interactive]. 2004, vol. 85(7), 1283–1285. Access via the Internet: <https://dx.doi.org/10.1063/1.1776621>.

28. OYSTON, S., et al. New 2,5-diaryl-1,3,4-oxadiazole–fluorene hybrids as electron transporting materials for blended-layer organic light emitting diodes. *Journal of Materials Chemistry* [interactive]. 2005, vol. 15(1), 194–203. Access via the Internet: <https://dx.doi.org/10.1039/b413066a>.

29. UOYAMA, H., et al. Highly efficient organic light-emitting diodes from delayed fluorescence. *Nature* [interactive]. 2012, vol. 492(7428), 234–238. Access via the Internet: <https://dx.doi.org/10.1038/nature11687>.

30. DIAS, F.B., et al. Triplet harvesting with 100% efficiency by way of thermally activated delayed fluorescence in charge transfer OLED emitters. *Advanced*

Materials [interactive]. 2013, vol. 25(27), 3707–3714. Access via the Internet: <https://dx.doi.org/10.1002/adma.201300753>.

31. SANTOS, P.L., et al. Engineering the singlet–triplet energy splitting in a TADF molecule. *Journal of Materials Chemistry C* [interactive]. 2016, vol. 4(17), 3815–3824. Access via the Internet: <https://dx.doi.org/10.1039/C5TC03849A>.

32. NOBUYASU, R.S., et al. Rational design of TADF polymers using a donor-acceptor monomer with enhanced TADF efficiency induced by the energy alignment of charge transfer and local triplet excited states. *Advanced Optical Materials* [interactive]. 2016, vol. 4(4), 597–607. Access via the Internet: <https://dx.doi.org/10.1002/adom.201500689>.

33. ZHANG, Q., et al. Design of efficient thermally activated delayed fluorescence materials for pure blue organic light emitting diodes. *Journal of the American Chemical Society* [interactive]. 2012, vol. 134(36), 14706–14709. Access via the Internet: < https://dx.doi.org/10.1021/ja306538w>.

34. TAO, Y., et al. Thermally activated delayed fluorescence materials towards the breakthrough of organoelectronics. *Advanced Materials* [interactive]. 2014, vol. 26(47), 7931–7958. Access via the Internet: <https://doi.org/10.1002/adma.201402532>.

35. DATA, P., and TAKEDA, Y. Recent advancements in and the future of organic emitters: TADF- and RTP-active multifunctional organic materials. *Chemistry – An Asian Journal* [interactive]. 2019, vol. 14(10), 1613 –1636. Access via the Internet: <https://doi.org/10.1002/asia.201801791>.

36. JI, Y., et al. Polymorphism-dependent aggregation-induced emission of pyrrolopyrrole-based derivative and its multi-stimuli response behaviors. *Dyes and Pigments* [interactive]. 2017, vol. 139, 664–671. Access via the Internet: <https://doi.org/10.1016/j.dyepig.2016.12.061>.

37. LEI, Y., et al. Polymorphism and mechanochromism of N-alkylated 1,4-dihydropyridine derivatives containing different electron-withdrawing end groups. *Journal of Materials Chemistry C* [interactive]. 2017, vol. 5(21), 5183–5192. Access via the Internet: <https://doi.org/10.1039/c7tc00362e>.

38. DONG, J., et al. Activation and tuning of green fluorescent protein chromophore emission by alkyl substituent-mediated crystal packing. *Journal of the American Chemical Society* [interactive]. 2009, vol. 131(2), 662–670. Access via the Internet: <https://doi.org/10.1021/ja806962e>.

39. BABU, S. S., et al. Excited state processes in linear π-system-based organogels. *The Journal of Physical Chemistry Letters* [interactive]. 2010, vol. 1(23), 3413–3424. Access via the Internet: <https://doi.org/10.1021/jz101219y>.

40. CHI, Z., et al. Recent advances in organic mechanofluorochromic materials. *Chemical Society Reviews* [interactive]. 2012, vol. 41(10), 3878–3896. Access via the Internet: <https://doi.org/10.1039/c2cs35016e>.

41. YAGAI, S., et al. Mechanochromic luminescence based on crystal-to-crystal transformation mediated by a transient amorphous state. *Chemistry of Materials* [interactive]. 2015, vol. 28(1), 234–241. Access via the Internet: <https://doi.org/10.1021/acs.chemmater.5b03932>.

42. XUE, P., et al. Recent progress in the mechanochromism of phosphorescent organic molecules and metal complexes. *Journal of Materials Chemistry C* [interactive]. 2016, vol. 4(28), 6688–6706. Access via the Internet: <https://doi.org/10.1039/c6tc01503d>.

43. HLADKA, I., et al. W-shaped bipolar derivatives of carbazole and oxadiazole with high triplet energies for electroluminescent devices. *Dyes and Pigments* [interactive]. 2018, vol. 149, 812–821. Access via the Internet: <https://doi.org/10.1016/j.dyepig.2017.11.043>.

44. SPARTAN'14 for windows version 1.1.4. 1840 Von Karman avenue, suite 370, Irvine, ca 92612. Wavefunction, Inc.; 2013.

45. ZHANG, D., et al. Highly efficient blue thermally activated delayed fluorescent OLEDs with record-low driving voltages utilizing high triplet energy hosts with small singlet–triplet splittings. *Chemical Science* [interactive]. 2016, vol. 7(5), 3355–3363. Access via the Internet: <https://doi.org/10.1039/c5sc04755b>.

46. REIG, M., et al. Tuning the ambipolar charge transport properties of tricyanovinyl-substituted carbazole-based materials. *Physical Chemistry Chemical Physics* [interactive]. 2017, vol. 19(9), 6721–6730. Access via the Internet: <https://doi.org/10.1039/c6cp08078b>.

47. HLADKA, I., et al. Polymorphism of derivatives of *tert*-butyl substituted acridan and perfluorobiphenyl as sky-blue OLED emitters exhibiting aggregation induced thermally activated delayed fluorescence. *Journal of Materials Chemistry C* [interactive]. 2018, vol. 6(48), 13179–13189. Access via the Internet: <https://doi.org/10.1039/c8tc04867c>.

48. ZHANG, L., et al. Aggregation-induced emission enhancement and aggregation-induced circular dichroism of chiral pentaphenylpyrrole derivatives and their helical self-assembly. *New Journal of Chemistry* [interactive]. 2017, vol. 41(17), 8877–8884. Access via the Internet: <https://doi.org/10.1039/c7nj00583k>.

49. STAKHIRA, P., et al. (2012). Blue organic light-emitting diodes based on pyrazoline phenyl derivative. *Synthetic Metals* [interactive]. 2012, vol. 162(3-4), 352–355. Access via the Internet: <https://doi.org/10.1016/j.synthmet.2011.12.017>.

50. Potopnyk, M. A., et al. Benzo[4,5]thiazolo[3,2-*c*][1,3,5,2]oxadiaza-borinines: synthesis, structural, and photophysical properties. *The Journal of Organic*

Chemistry [interactive]. 2018, vol. 83(19), 12129–12142. Access via the Internet: <https://doi.org/10.1021/acs.joc.8b02098 >.

51. Potopnyk, M. A., et al. Application of the Suzuki−Miyaura reaction for the postfunctionalization of the benzo[4,5]thiazolo[3,2-*c*][1,3,5,2]oxadiazaborinine core: an approach toward fluorescent dyes. *The Journal of Organic Chemistry* [interactive]. 2019, vol. 84(9), 5614−5626. Access via the Internet: <https://doi.org/10.1021/acs.joc.9b00566 >.

52. CHAPRAN, M., et al. An ambipolar BODIPY derivative for a white exciplex OLED and cholesteric liquid crystal laser toward multifunctional devices. *ACS Applied Materials & Interfaces* [interactive]. 2017, vol. 9(5), 4750–4757. Access via the Internet: <https://doi.org/10.1021/acsami.6b13689>.

53. RAO, Y.-L., and WANG, S. Four-coordinate organoboron compounds with a π-conjugated chelate ligand for optoelectronic applications. *Inorganic Chemistry* [interactive]. 2011, vol. 50(24), 12263–12274. Access via the Internet: <https://doi.org/10.1021/ic200658v>.

54. ZHANG, X., et al. Star-shaped carbazole-based BODIPY derivatives with improved hole transportation and near-infrared absorption for small-molecule organic solar cells with high open-circuit voltages. *RSC Advances* [interactive]. 2015, vol. 5(41), 32283–32289. Access via the Internet: <https://doi.org/10.1039/c5ra02414e>.

55. LOUDET, A., and BURGESS, K. BODIPY dyes and their derivatives: syntheses and spectroscopic properties. *Chemical Reviews* [interactive]. 2007, vol. 107(11), 4891–4932. Access via the Internet: <https://doi.org/10.1021/cr078381n>.

6. CURRICULUM VITAE

Name, Surname:	Iryna Hladka
Birth date	December 01, 1993
E-mail:	ira.hladka@gmail.com

Education

2010–2014	Bachelor's Degree in Chemistry, Ivan Franko National University of Lviv, Chemistry Faculty, Ukraine
2014–2015	Master's Degree in Chemistry, Ivan Franko National University of Lviv, Chemistry Faculty, Ukraine
2015–2019	PhD studies in Materials Engineering, Kaunas University of Technology, Faculty of Chemical Technology

Work experience

May 02, 2016 – May 31, 2016	The European Community's 7th Framework Programme project "Centre of Excellence in Organic Semiconductors Research" (CEOSeR). Project junior researcher. Kaunas University of Technology, Department of Polymer Chemistry and Technology
April 01, 2017 – December 31, 2017	Project "Influence of structure properties of organic solid-state emitters on their thermally activated delayed fluorescence efficiency (X-ray TADF)". Project junior researcher. Kaunas University of Technology, Department of Polymer Chemistry and Technology
September 23, 2019– present	Project "Vertical organic light-emitting transistors based on thermally-activated-delayed-fluorescence emitters". Project junior researcher. Kaunas University of Technology, Department of Polymer Chemistry and Technology

Internships

November 11, 2015 – December 11, 2015	Lviv Polytechnic National University, Ukraine. FP7-PEOPLE-2013-IRSES project "Multicoloured ambipolar conducting polymers for single polymer optoelectronic devices" (AmbiPOD).

7. LIST OF PUBLICATIONS

Papers in the journals inscribed in the list approved by the Institute for Scientific Information (ISI):

1. **Hladka, I.**, Lytvyn, R., Volyniuk, D., Gudeika, D., Grazulevicius, J.V. W-Shaped Bipolar Derivatives of Carbazole and Oxadiazole with High Triplet Energies for Electroluminescent Devices // Dyes and Pigments. 2018, vol. 149, pp. 812–821.
2. **Hladka, I.**, Volyniuk, D., Bezvikonnyi, O., Kinzhybalo, V., Bednarchuk, T.J., Danyliv, Y., Lytvyn, R., Lazauskas, A., Grazulevicius, J.V. Polymorphism of Derivatives of *tert*-Butyl Substituted Acridan and Perfluorobiphenyl as Sky-Blue OLED Emitters Exhibiting Aggregation Induced-Active Thermally Activated Delayed Fluorescence. Journal of Materials Chemistry C. 2018, vol. 6 (48), pp. 13179–13189.
3. Potopnyk, M.A., Volyniuk, D., Ceborska, M., Cmoch, P., **Hladka, I.**, Danyliv, Y., Grazulevicius, J.V. Benzo[4,5]thiazolo[3,2-c][1,3,5,2]oxadiazaborinines: Synthesis, Structural and Photophysical Properties. The Journal of Organic Chemistry. 2018, vol. 83 (19), pp. 12129–12142.
4. Potopnyk, M.A., Volyniuk, D., Luboradzki, R., Ceborska, M., **Hladka, I.**, Danyliv, Y., Grazulevicius, J.V. Application of the Suzuki-Miyaura Reaction for the Postfunctionalization of the Benzo[4,5]thiazolo[3,2-c][1,3,5,2]oxadiazaborinine Core: An Approach towards Fluorescent Dyes. The Journal of Organic Chemistry. 2019, vol. 84 (9), pp. 5614–5626.

Attendance of international conferences:

1. **Hladka, Iryna**; Volyniuk, Dmytro; Bezvikonnyi, Oleksandr; Lytvyn, Roman; Grazulevicius, Juozas V. Derivatives of 9,9-dimethyl-9,10-dihydroacridine and perfluorobiphenyl as emitters showing thermally activated delayed fluorescence // *ICOM 2018: 5th international conference on the physics of optical materials and devices*, Igalo, Montenegro, August 27 – August 31, 2018: book of abstracts. Beograd: Institut za nuklearne nauke "Vinča", 2018. ISBN 9788673061412, p. 141.
2. **Hladka, Iryna**; Lytvyn, Roman; Bezvikonnyi, Oleksandr; Volyniuk, Dmytro; Gražulevičius, Juozas Vidas. Octafluorobiphenyl as new acceptor for the synthesis of bipolar compounds with negligible singlet-triplet energy splitting // *Baltic polymer symposium 2017*: Tallinn, Estonia, September 20–22, 2017 / Co-organized by Tallinn University of Technology and COST action CA15107. Tallinn: TTU. 2017, p. 115.
3. **Hladka, Iryna**; Lytvyn, Roman; Bezvikonnyi, Oleksandr; Volyniuk, Dmytro; Gražulevičius, Juozas Vidas. Bipolar oxadiazole derivatives with high triplet energies // *Advanced materials and technologies*: book of abstracts of the 19th international conference-school, August 27–31, 2017, Palanga, Lithuania. Kaunas: Kaunas University of Technology. ISSN 1822-7759. 2017, P52, p. 77.
4. **Hladka, Iryna**; Lytvyn, Roman; Bezvikonnyi, Oleksandr; Volyniuk, Dmytro; Gražulevičius, Juozas Vidas. Nonafluorobiphenyl as new and promising aceptor

unit in design of TADF emitters // *State of the Art in Organic-only TADF OLEDs. From Theory to Applications*: XXIInd International Krutyn Summer School 2017 Krutyń, Masurian Lake District, Poland, May 21–27, 2017 / 2017, p. 44.

5. **Hladka, Iryna**; Lytvyn, Roman; Volyniuk, Dmytro; Pečiulytė, Laura; Gražulevičius, Juozas Vidas. Synthesis and photophysical properties of tetraarylpyrrole and diphenylphosphine oxide conjugates // *Baltic polymer symposium 2016*: Klaipėda, September 21–24, 2016: programme and abstracts / Kaunas University of Technology, Vilnius University, Klaipėda University. Kaunas: Kaunas University of Technology, 2016. ISBN 9786090212356, p. 82.
6. **Hladka, Iryna**; Lytvyn, Roman; Bagdžiūnas, Gintautas; Danyliv, Yan; Volyniuk, Dmytro; Gražulevičius, Juozas Vidas. Bipolar organic semiconductors containing carbazole and oxadiazole units // *Molecular crystals and liquid crystals: the jubilee 10th international conference on electronic processes in organic and inorganic materials*, ICEPOM-10, May 23–27, 2016, Ternopol, Ukraine. Oxon: Taylor & Francis. ISSN 1542-1406. 2016, p. 71.

8. ACKNOWLEDGMENTS

Prof. Habil. Dr. Juozas Vidas Gražulevičius (Department of Polymer Chemistry and Technology, Kaunas University of Technology) is sincerely thanked for the supervision of my Doctoral Research, consultations, valuable advice and great support.

Dr. Dmytro Volyniuk (Department of Polymer Chemistry and Technology, Kaunas University of Technology) is kindly thanked for the advising of my work, friendship, measurements of charge-transporting, photoelectron emission properties, OLEDs characteristics, for sharing knowledge in photophysics and for valuable scientific discussion.

Dr. Yan Danyliv (Department of Polymer Chemistry and Technology, Kaunas University of Technology) is heartily acknowledged for support, for sharing knowledge in theoretical calculations, and for invaluable ideas, advice and interesting scientific discussion.

Mrs. Galyna Sych (Department of Polymer Chemistry and Technology, Kaunas University of Technology) is greatly thanked for friendship, help and highly applicable advice and entertaining discussions.

Dr. Jūrate Simokaitienė (Department of Polymer Chemistry and Technology, Kaunas University of Technology) is thanked for the measurements of thermal properties.

All the colleagues of the research group are thanked for their help and friendly working atmosphere.

Finally, I render my thankfulness to my family for their faith in me and great moral support.

SL344. 2020-01-27. 7,25 leidyb. apsk. l. Tiražas 12 egz.
Išleido Kauno technologijos universitetas, K. Donelaičio g. 73, 44249 Kaunas
Spausdino leidyklos „Technologija“ spaustuvė, Studentų g. 54, 51424 Kaunas